

## 2022 SGK-SSCr Meeting – Final Programme



Scientific Programme

### Annual Meeting Swiss Society for Crystallography

15 September 2022

**u<sup>b</sup>** UNIVERSITÄT BERN

08:30		Registration & <b>coffee</b>
09:20	Simon Grabowsky and Norbert Polacek	Welcome address
09:30 – 10:30	Chairs: Sergey Churakov and Georgia Cametti	<b>Materials and minerals</b>
09:30 – 10:00	Invited speaker: Enrico Mugnaioli	3D electron diffraction applied to complex nanoparticles and nanominerals
10:00 – 10:15	Aurelio Borzi	Microstructure and lattice defects in epitaxial Pt thin films
10:15 – 10:30	Ilia Kochetygov	Controlling structure and dimensionality of metal-organic frameworks using N-heterocyclic and counterion chemistry
10:30 – 11:00		<b>Coffee break, posters and sponsors</b>
11:00 – 12:00	Chair: Paula Abdala	<b>Large user facilities in Switzerland</b>
11:00 – 11:12	Nicola Casati	Swiss Light Source
11:12 – 11:24	Dmitry Chernyshov	Swiss Norwegian Beamlines, ESRF
11:24 – 11:36	Céline Besnard	Dubochet Center for Imaging
11:36 – 11:48	Bill Pedrini	SwissFEL
11:48 – 12:00	Romain Sibille	Laboratory for Neutron Scattering and Imaging
12:00 – 12:30	Chair: Pascal Schouwink	<b>Round table discussion on future SSCr workshops</b>
12:30 – 14:30		<b>Lunch, posters and sponsors</b>
13:30 – 14:30	for SSCr members	<b>SSCr Annual General Assembly</b>
14:30 – 15:30	Chair: Achim Stocker	<b>Structural biology</b>
14:30 – 15:00	Invited speaker: Andreas Engel	Cryo electron microscopy of 2D crystals and single particles
15:00 – 15:15	Natercia Barbosa	Combined in vitro and in vivo investigation of barite biomineralization in Spirogyra
15:15 – 15:30	Leonard Krupnik	Illuminating the structure of iron carbohydrates in complex biological environments
15:30 – 16:00		<b>Coffee break, posters and sponsors</b>
16:00 – 17:00	Chairs: Hans-Beat Bürgi and Lorraine Malaspina	<b>Chemical crystallography</b>
16:00 – 16:30	Invited speaker: Simon Parsons	Studying polymorph evolution with electron diffraction
16:30 – 16:45	Yevheniia Kholina	Tuning local structure in Prussian Blue Analogues
16:45 – 17:00	Ariel F. Perez Mellor	Solid-state synthesis of cyclo Leu-Leu: zwitterionic form vs trifluoroacetic acid salt
17:00		<b>Poster prize and farewell apéro</b>



<https://landing.eldico-scientific.com/the-future-of-crystallography-is-here>



<https://www.bruker.com/de/products-and-solutions/diffractometers-and-scattering-systems/single-crystal-x-ray-diffractometers.html>



<https://www.dectris.com/>



**Malvern  
Panalytical**  
a spectris company

<https://www.malvernpanalytical.com/en>



**Rigaku**

<https://www.rigaku.com/>



<https://www.stoe.com/>

## 2022 SGK-SSCr Meeting – Abstracts : I - Invited plenaries

# 3D electron diffraction applied to complex nanoparticles and nanominerals

Talk  
1

Enrico Mugnaioli (1), Mauro Gemmi (2)

(1) *Dipartimento di Scienze della Terra, Università di Pisa, Pisa, Italy.* (2) *Center for Materials Interfaces, Electron Crystallography, Istituto Italiano di Tecnologia, Pontedera (PI), Italy.*

Electron diffraction has been long regarded as a purely quantitative method, due to poor accuracy and dynamical effects. Yet, in the late 2000's the first attempts to collect single-crystal electron diffraction data and to use them for ab-initio structure determination revealed unexpectedly successful [1]. In the following ten years, the method has attracted the attention of mineralists, chemists, material scientists and structural biologists, because it has proved able to cover the missing gap between the smallest crystals tractable with X-rays (1-50  $\mu\text{m}$ ) and the smallest crystalline seeds (10-100 nm) [2].

The so-called 3D electron diffraction method is very efficient with organic compounds and macromolecules despite their beam sensitivity, but is especially powerful for inorganic materials. In fact, it is possible to collect reliable structural data from particles and areas as small as few tens of nanometers. Here we will show the recent characterization of a series of sub-micrometric crystalline phases found in corundum grains from Luobusa ophiolite, Tibet, China [3-4] (Figure 1). A rich collection of unexpected new minerals was discovered inside a handful of FIB lamellae. Moreover, we will display that 3D electron diffraction can be used for the structural characterization of complex synthetic nanoparticle systems [5-6], possibly besting more established crystallographic methods like powder X-ray diffraction and high-resolution (S)TEM imaging.

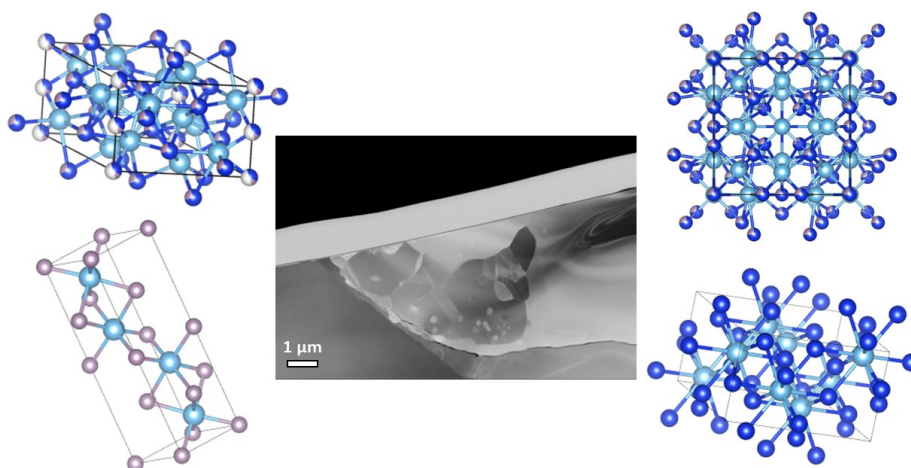


Figure 1- FIB lamella from Luobusa ophiolite, containing four new minerals, whose structures are sketched on side.

- [1] Rozhdestvenskaya, Mugnaioli, et al. *Mineralogical Magazine* 74 (2010): 159-177.
- [2] Gemmi, Mugnaioli, et al. *ACS Central Science* 5 (2019): 1315-1329.
- [3] Xiong, Xu, et al. *European Journal of Mineralogy* 32 (2020): 557-574.
- [4] Xiong, Xu, et al. *American Mineralogist*, doi: 10.2138/am-2022-8226.
- [5] Kaiukov, Almeida, et al. *Inorganic Chemistry* 59 (2020): 548-554.
- [6] Toso, Akkerman, et al. *Journal of the American Chemical Society* 142 (2020): 10198-10211.

# Cryo electron microscopy of 2D crystals and single particles

Talk  
9

Andreas Engel

*Emeritus, University of Basel*

Electron microscopy (EM) introduced a fast and lasting change to biological and biomedical research and is radically changing the drug discovery process. Direct electron detector cameras and improved image processing algorithms now allow the structure determination of large biomolecules by cryogenic EM (cryo-EM) at atomic resolution using a single particle approach. Thus, cryo-EM has become the most successful method to acquire atomic structure information of biomacromolecule and is applied in basic research and industry worldwide. Historically, cryo-EM was the first method to unveil the basic structure of a membrane protein in 1975, exploiting the crystalline arrangement of bacteriorhodopsin in the purple membrane. Other membrane protein structures followed, mainly from artificial 2D crystals reconstituted from lipids and purified membrane proteins kept in solution by detergents. Crystallization experiments were not always successful and electron crystallography did not become an easy-to-use method. However, sample vitrification protocols and amazing progress in cryo-EM technology makes it possible today to assess the atomic structure of >50 kDa biomolecules without the prerequisite of 2D or 3D crystals.

## Studying polymorph evolution with electron diffraction

Talk  
12

Edward T. Broadhurst (1), Hongyi Xu (2), Xiaodong Zou (2), Fabio Nudelman (1) and Simon Parsons (1)

[1] School of Chemistry, The University of Edinburgh, UK. (2) Department of Materials and Environmental Chemistry, Stockholm University, Sweden.

There is a huge amount of current interest in crystallographic applications of transmission electron microscopy (TEM) and microcrystal electron diffraction. Many papers in this rapidly developing field show how the very strong interaction of electrons with matter can be used to obtain crystal structures from samples which are orders of magnitude smaller than those used for X-ray diffraction. This contribution will describe application of these techniques to monitor a dynamic process, the evolution of different polymorphic forms of organic materials during crystal growth. Glycine has three known polymorphs ( $\alpha$ ,  $\beta$  and  $\gamma$ ) at ambient conditions. Crystal growth can be halted after time periods of between 3 and 6 minutes to show that these polymorphs appear successively[1]. The thermodynamically least stable  $\beta$  polymorph forms exclusively after 3 minutes, but this begins to yield to the better-known  $\alpha$ -form after just one minute more, with one crystallite of the  $\gamma$  form being observed after an hour. A second study, this time on carbamazepine[2], revealed the formation of no less than four different solid forms from a single solution after just 30 s of crystal growth. After 20 s, only droplet-like particles are observed, which were shown to be a precursor phase of carbamazepine dehydrate, forming via a phase separation mechanism. In all but one case, the crystal structures of each form of glycine and carbamazepine could be determined from the electron diffraction data. These results show that multiple polymorphs can be rapidly identified and their crystal structures determined from a single sample, even if they are present in vanishingly small quantities. This technique has the potential greatly to accelerate polymorph discovery in pharmaceuticals and other applications where specific solid forms of materials are required.

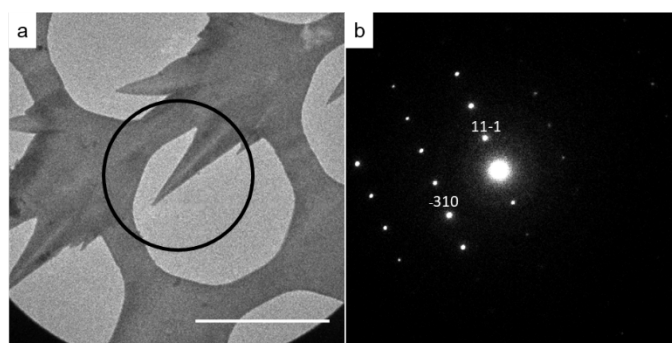


Figure 2: (a) Crystals of  $\beta$ -glycine on a TEM grid after 3 minutes of crystal growth, and (b) a corresponding electron diffraction image. The scale bar in (a) indicates 3  $\mu\text{m}$ .

[1] Broadhurst, Xu, Clabbers, Lightowler, Nudelman, Zou, and Parsons. IUCrJ 7 (2020): 5-9.

[2] Broadhurst, Xu, Nudelman, and Parsons. IUCrJ 8 (2021): 860-866.

## 2022 SGK-SSCr Meeting – Abstracts : II - Oral contributions

## Microstructure and lattice defects in epitaxial Pt thin films: comparison between conventional RF sputtering and facing target cathode depositions

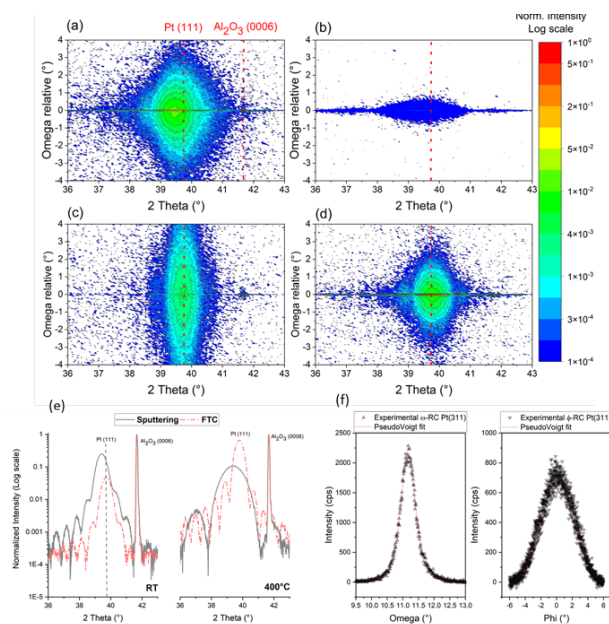
Aurelio Borzi<sup>a</sup>, Simone Dolabella<sup>a,b</sup>, Alex Dommann<sup>a</sup>, Antonia Neels<sup>a,b</sup>

<sup>a</sup>Center for X-ray Analytics, Swiss Federal Laboratories for Materials Science and Technology, Empa, Überlandstrasse 129, CH-8600 Dübendorf, Switzerland

<sup>b</sup>Department of Chemistry, University of Fribourg, Chemin du Musée 9, 1700 Fribourg, Switzerland

Platinum thin films are exploited in many applications where high-temperature and corrosion-resistance are required. Pt thin layers can be obtained by MBE when high crystalline perfection is required, or conventional RF sputtering to increase the growth rate. A novel deposition method, Facing Target Cathode (FTC), provide adatoms with kinetic energies lower than RF sputtering, but higher growth rates than MBE, potentially enabling the deposition of highly epitaxial Pt thin films at an acceptable growth rate. In this study [1], we used high-resolution X-ray diffraction (HRXRD) [2] to compare the microstructure Pt thin films deposited by FTC and conventional RF sputtering. Orientations and texture, lattice strain, mosaicity, and dislocation densities have been evaluated and correlated with the deposition parameters, especially the substrate temperature. HRXRD investigations confirmed that FTC allows the deposition of highly epitaxial Pt thin films with low strain and defects densities, and smooth surfaces, through optimizing the substrate temperature.

Figure 1. (a) and (b) RSMs around the Pt 111 and c-sapphire 006 lattice points in Pt thin film deposited by conventional RF sputtering and FTC; (c) XRD Radial scans of the Pt 111 and c-sapphire 006 for different deposition methods and parameters. (f) Omega and Phi rocking curves collected to verify the epitaxial nature of the Pt thin films and estimate the dislocations densities.



[1] O. Yıldırım *et al.*, «Tuning the microstructure of the Pt layers grown on Al<sub>2</sub>O<sub>3</sub> (0001) by different sputtering methods», *Scripta Materialia*, vol. 194, pag. 113689, mar. 2021, doi: 10.1016/j.scriptamat.2020.113689.

[2] S. Dolabella, A. Borzi, A. Dommann, e A. Neels, «Lattice Strain and Defects Analysis in Nanostructured Semiconductor Materials and Devices by High-Resolution X-Ray Diffraction: Theoretical and Practical Aspects», *Small Methods*, pag. 2100932, dic. 2021, doi: 10.1002/smt.202100932.

# Controlling structure and dimensionality of metal-organic frameworks using N-heterocyclic and counterion chemistry

Talk  
3

Ilia Kochetygov (1,2), Mehrdad Asgari (1,3), Anita Justin (1), Wendy L. Queen (1)

[1] Institute of Chemical Sciences and Engineering, École Polytechnique Fédérale de Lausanne (EPFL), CH-1951 Sion, Switzerland

[2] Paul Scherrer Institut, 5232 Villigen, Switzerland

[3] Department of Chemical Engineering & Biotechnology, University of Cambridge, Philippa Fawcett Drive, Cambridge CB3 0AS, UK

Metal-organic frameworks (MOFs) are rising stars among nano- and micro-porous materials due to their intrinsic tunability and structural versatility leading to a host of applications including but not limited to gas separation and storage, catalysis, etc. Through a prudent selection of two main MOF building blocks that are metal clusters and organic ligands, new materials with tailor-made functionalities can be produced. N-heterocyclic carbene (NHC) ligands, being versatile and stable carbenes, might grant MOFs new catalytic activity in hydrogenation and attractive properties in CO<sub>2</sub> capture. Based on the distinct success of solution-based NHC chemistry for the aforementioned applications, as well as established principles of ligand design, we aim our efforts at synthesizing MOFs constructed by novel ligands that are bearing NHC functionality. We show that with a given NHC ligand, **H<sub>2</sub>Sp5-BF<sub>4</sub>**, two different MOF structures can be obtained in a controlled manner by choosing an appropriate counterion in the MOF synthesis, namely **Cu-Sp5**<sup>[1]</sup> and **Cu-Sp5-BF<sub>4</sub>**<sup>[2]</sup> (Figure 1). We show that in the former structure, a synergistic combination of open metal sites and charged backbone leads to the top values of CO<sub>2</sub>/N<sub>2</sub> selectivity in flue gas conditions. The latter structure is shown to undergo a series of structural transformations to form a turbostratic phase. We show these transformations enhance NHC site accessibility and allow for post-synthetic metalation with iridium on carbene centers. The catalytic activity of the iridium-modified material is demonstrated in a stilbene hydrogenation reaction.

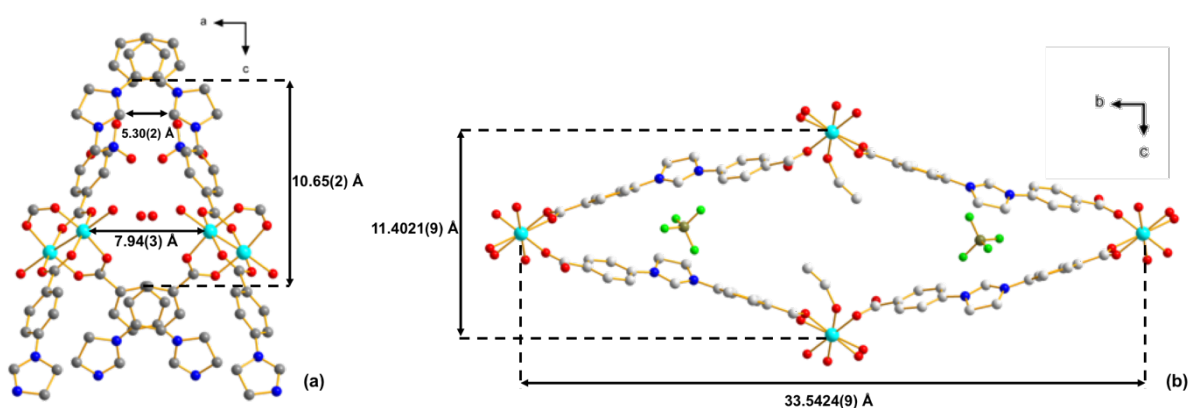


Figure 3. (a) Cu-Sp5 and (b) Cu-Sp5-BF<sub>4</sub> structures

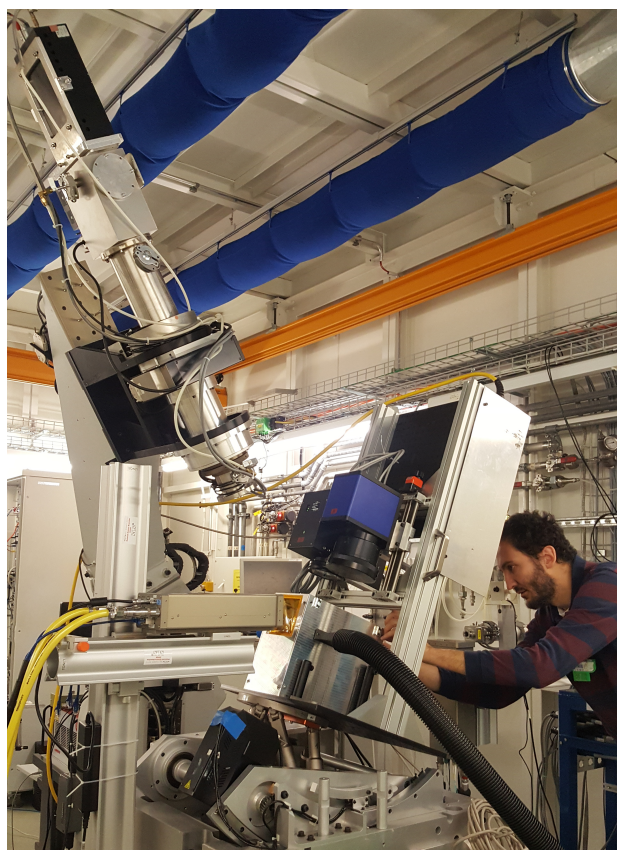
[1] I. Kochetygov, S. Bulut, M. Asgari, W. L. Queen, *Dalt. Trans.* **2018**, 47, 10527–10535.

[2] I. Kochetygov, A. Justin, M. Asgari, S. Yang, V. Karve, T. Schertenleib, D. Stoian, E. Oveisi, M. Mensi, W. L. Queen, *Chem. Sci.* **2022**, 13, 6418–6428.

Nicola Casati (1)

[1] Paul Scherrer Institute, Laboratory for Synchrotron Radiation – Condensed Matter, Forschungstrasse 111, 5232 Villigen

Several stations offer diffraction capabilities at the SLS. Diffraction is a complementary technique at SuperXAS, Debye, microXAS, cSAXS as well as Phoenix. The Materials Science



beamline is instead fully dedicated to advanced diffraction studies operated on three separate experimental tables.<sup>1</sup> From high-resolution XRPD to single crystal, diffuse scattering, surface diffraction, fast time-resolved and very high-throughput measurements, the station offers numerous possibilities for advanced crystallographic studies. The stations are very versatile for both industrial and academic users, with a broad span of user communities. A recently appointed new scientist is taking care of upgrading the third table, which is also equipped with a standard X-ray tube for offline measurements.

All beamlines will retain/expand their diffraction capabilities. The Materials Science beamline, in particular, will be named ADDAMS after the SLS 2.0 upgrade, with new specs and equipment available and planned. The present as well as the future status and plans will be discussed.

Figure 4- Setup for 22 kHz diffraction on the third diffractometer.

[1] P.R. Willmott *et al.* *J. Synchrotron Rad.* (2013). 20, 667–682

## Swiss-Norwegian Beam Lines at the European Synchrotron Radiation Facility – a current status and near future

Talk  
5

Dmitry Chernsyhov, Vadim Dyadkin, Dragos Stoian, and Wouter van Beek

*[1] Swiss-Norwegian Beam Lines at European Synchrotron Radiation Facility, 38000 Grenoble, France*

SNBL provides synchrotron instruments for material research on two beamlines. Illustrations from recent user's experiments will be presented with emphasis on the power of combination of various scattering techniques. We also present on-going developments on hardware and software that offer unique opportunities to study their fascinating materials and complex physical and chemical processes in an efficient and user friendly manner.

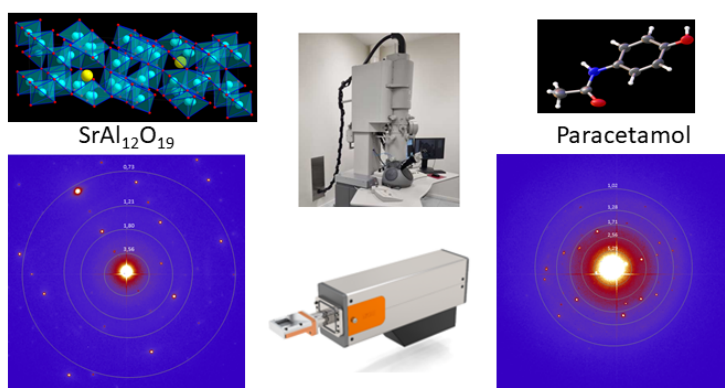
## Implementing a service of 3D-ED at the Dubochet Center for Imaging Geneva.

Talk  
6

Maxime Patigniez (1,2), Yashar Sadian (3), Céline Besnard(1,3)

[1] Department of Molecular Biology, University of Geneva [2] Laboratoire de cristallographie, University of Geneva (3) Dubochet Center for Imaging, Geneva.

3D electron diffraction or microcrystal electron diffraction (MicroED) has emerged as a promising technique for structure elucidation of small crystals [1]. The Dubochet Center for Imaging in Geneva recently acquired a new hybrid pixel detector from Amsterdam Scientific in order to enable the collection of high-quality 3D-electron diffraction data. We will introduce you to our journey into the implementation of the 3D electron diffraction service at the DCI Geneva, focussing on the experimental set-up, the sample preparation and the data quality.



[1] Gemmi Mauro, et al. ACS Cent Sci.. 5(8) (2019) :1315-1329.

# Crystallography at SwissFEL: Instrumentation and scientific opportunities

Talk  
7

Bill F. Pedrini

*Paul Scherrer Institut, 5232 Villigen PSI, Switzerland*

The Swiss Free Electron X-ray Laser provides ultrashort, high-intensity pulses in the soft and hard x-ray wavelength range. Currently, three experimental stations are in user operation and two in the commissioning phase. The talk aims to present the features of the SwissFEL pulses as well as the instrumentation available at the different experimental station, shedding light on the possibilities and opportunities for x-ray crystallography at the SwissFEL.

Romain Sibille, Oksana Zaharko, Lukas Keller, Vladimir Pomjakushin,  
Denis Sheptyakov and Jonathan White (1)

[1] *Laboratory for Neutron Scattering & Imaging, Paul Scherrer Institut, 5232 Villigen PSI, Switzerland.*

In a number of cases, neutron crystallography can offer major advantages to characterize materials of various kinds, for both their nuclear and magnetic structures. We quickly review some of the experimental capabilities for powder and single-crystal neutron diffraction at the Swiss spallation neutron source SINQ [1] (Figure 1): the thermal neutron diffractometers ZEBRA (single crystals) and HRPT (powders), the cold neutron diffractometer DMC, and the small angle neutron scattering instrument SANS-I. In particular, we present new directions for single-crystal samples, for efficient mapping of reciprocal space and for measurements on very small specimen.

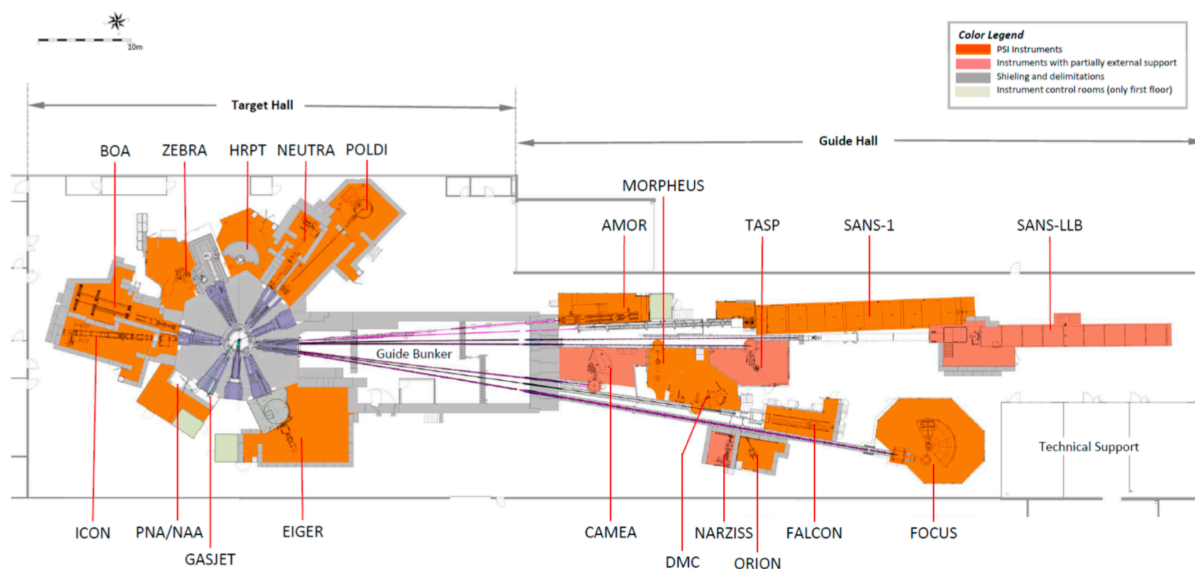


Figure 5- Layout of instruments at the Swiss neutron spallation source SINQ in 2020, after the facility upgrade [2].

[1] <https://www.psi.ch/en/lms-diffraction>

[2] Thomas, Geue, et al. *Swiss Neutron News (2021): 57, 6–15.*

## Combined *in vitro* and *in vivo* investigation of barite biomineralization in *Spirogyra*

Talk  
10

Natercia Barbosa (1), Jean-Michel Jaquet (2), Oscar Urquidi (1), Takuji B.M. Adachi (1), Montserrat Filella (3)

(1) Département de Chimie physique, Université de Genève, 1205 Genève, Suisse. (2) Département des Sciences de la Terre, Université de Genève, 1205 Genève, Suisse. (3) Département F.-A Forel des Sciences de l'environnement et de l'eau, Université de Genève, 1205 Genève, Suisse.

The geochemical cycle of barium in the environment has been of importance in multidisciplinary studies to obtain paleoclimate information. Interestingly, barite precipitation occurs in widely undersaturated conditions and its mechanism remains elusive. While the most accepted hypothesis of barite precipitation is the degradation of sinking organic matter creating barite-supersaturated microenvironments [1], barite biomineralization in green freshwater algae has been largely neglected. We have investigated the biomineralization of barite in a freshwater alga, *Spirogyra*, recognizable for its helical chloroplasts and known recently for its invasion in Lake Baikal [2]. Its ability of biomineralizing BaSO<sub>4</sub> microcrystals is yet often disregarded. Here, we characterized the size, morphology, and location of barite microcrystals in *Spirogyra* sp. by combining *in vitro* and *in vivo* experiments.

First, simply dried *Spirogyra* samples were imaged using scanning electron microscope (SEM) and energy-dispersive X-ray spectroscopy (EDXS). The number and size of barite microcrystals were found to be related to the barium concentration in the media. Cultures grown in a medium poor in barium showed less number and smaller size of crystals, while cultures grown in high concentrations of barium possessed more and bigger crystals. Additionally, their morphology showed a fast-growing face, (011), which is not normally observed. This suggests the influence of organic molecules on the growth kinetics. Snapshots of different stages of crystal growth could therefore be observed, before reaching the final rhombic morphology with (210) and (001) faces. Then, the critical point drying method was applied to preserve the internal and external structures of *Spirogyra* cells. This allowed us to observe more detailed structural information and the location of barite microcrystals by SEM imaging. Microcrystals were found against the cytoplasmic membrane, close to chloroplasts and fibrillary network. Finally, optical microscopy and Raman tweezer microspectroscopy were used to observe the microcrystals in living cells. Under a light microscope, many diffusing particles at micrometer scale were found at the top and bottom of the cell. Raman tweezer microspectroscopy was used to analyze the composition of the diffusing particles *in vivo*. The Raman spectra of trapped particles displayed sulfate peaks that were confirmed as barite from separate EDXS analyses. These barite microcrystals are thus optically visible and remarkably travel through the cell with the cytoplasmic streaming, implying their location in cytoplasm.

The combined *in vitro* and *in vivo* studies let us propose that barite formation in *Spirogyra* occurs in the cytoplasm where barium is supplied by non-selective but active transport of the divalent cations needed for actin polymerisation, while sulphate is needed for amino acid biosynthesis in chloroplasts [3]. This study lays a basis for investigating the question: why *Spirogyra* holds barite microcrystals intracellularly?

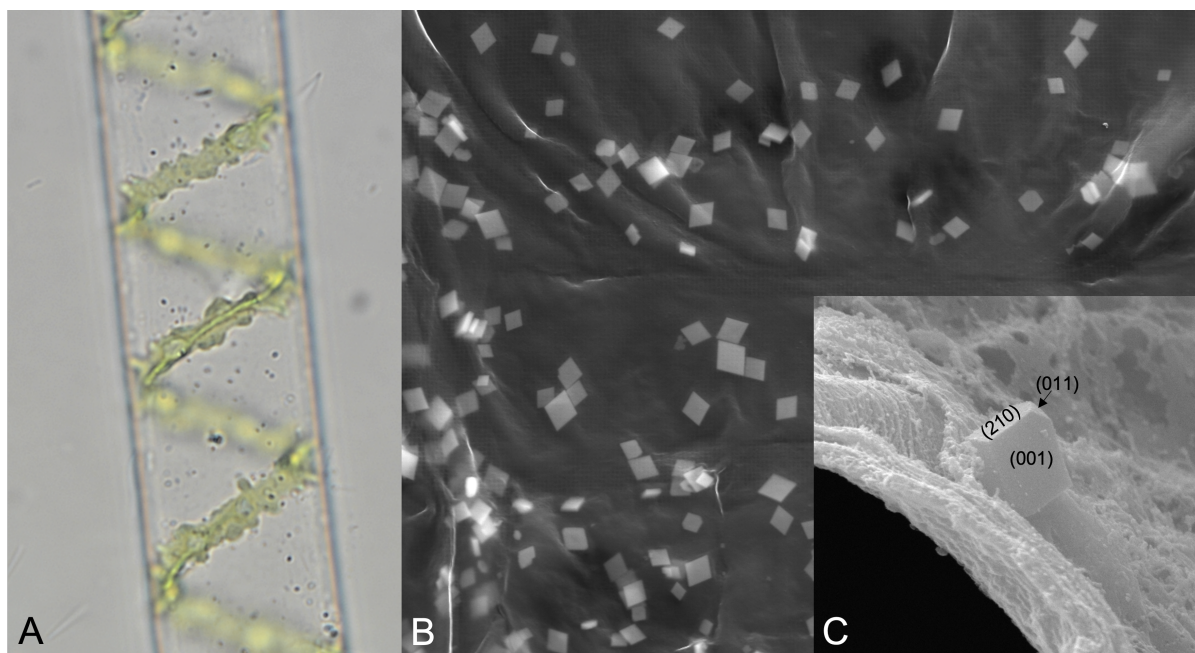


Figure 6- (A) Optical microscopy image of *Spirogyra* sp. focused at the bottom of the cell. Barite microcrystals corresponded to the black and white particles (B) SEM image of simply dried sample of *Spirogyra*. Barite microcrystals, with hexagonal and rhombic shape, appeared as bright particles under the cell wall. (C) SEM image of a *Spirogyra* sample dried from the critical point method. Barite microcrystal found against the cytoplasmic membrane and cell wall showing the characteristic rhombic crystal faces, (210) and (001), and the fast-growing one, (011).

- [1] Martinez-Ruiz, Francisca C., et al. *Chemical Geology* 511 (2019): 441-451.  
 [2] Vadeboncoeur, Yvonne, et al. *Bioscience* 71 (2021): 1011-1027.  
 [3] Barbosa, Natércia, Jaquet, Jean-Michel, Urquidi, Oscar, Adachi, Takuji B.M, Filella, Montserrat. *Journal of Plant Physiology* (2022):  
<https://doi.org/10.1016/j.jplph.2022.153769>.

# illuminating the structure of iron carbohydrates in complex biological environments

Talk  
11

Leonard Krupnik (1,2,3), Neda I. Anaraki (1,2,3), Marianne Liebi (4,5), Jonathan Avaro (1), Joachim Kohlbrecher (6), Peter Wick (2), Antonia Neels (1,3)

(1) Center for X-ray Analytics, Empa, Lerchenfeldstrasse 5, St. Gallen, 9014 Switzerland. (2) Particles-Biology Interactions Laboratory, Empa, Lerchenfeldstrasse 5, 9014, St. Gallen, Switzerland. (3) Department of Chemistry, University of Fribourg, Chemin du Musée 9, 1700, Fribourg, Switzerland. (4) Structure and Mechanics of Advanced Materials, PSI, Villigen, CH-5232, Switzerland. (5) Laboratory for X-ray characterization of materials, EPFL, CH-1015 Lausanne, Switzerland. (6) Laboratory for Neutron Scattering, PSI, Villigen, CH-5232, Switzerland.

Intravenous iron carbohydrate nanoparticles are widely used nanomedicines to treat iron deficiency anaemia, which is associated with illnesses such as chronic kidney disease and inflammatory bowel disease (1,2). A variety of clinical and biological studies on these products (ferric carboxymaltose and iron sucrose) are available (3); however, their undergoing structural changes during the early stages of entering the human bloodstream are not fully understood. Using a combination of small-angle x-ray and neutron scattering (SAXS/SANS), we investigated how size, shape and agglomeration of iron carbohydrates was influenced by interaction with proteins in the plasma. Hereby, SAXS was used to study the iron core, and was complemented by SANS to investigate the much weaker scattering signature of the carbohydrate shell. Our SAXS experiments indicated formation of agglomerates from single iron cores, which change their shape and size with increasing dilution in biological buffer. SANS measurements also enabled calculation of the thickness and shape of the carbohydrate shell. First experiments on interactions of iron sucrose with human serum albumin suggested adsorption of the protein to the NP surface after only 1h of incubation time. With this approach, we shine light on the correlation of physicochemical parameters of iron carbohydrates with their behavior in biological environments for better prediction of clinical outcomes.

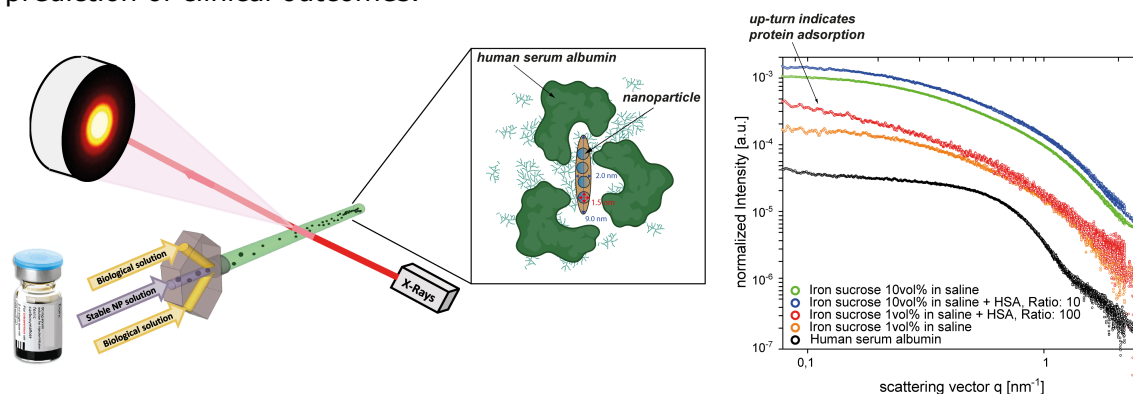


Figure 7 - Modelling the interaction between human serum albumin and iron sucrose through SAXS.

- [1] M. Prasherberger, et al., *Biomaterials*, 2015, 28(1), 35-50.
- [2] J. Rottembourg, et al., *Nephrology Dialysis Transplantation*, 2011, 26(10), 3262-3267.
- [3] N. Nikravesh, et al., *Nanomedicine: Nanotechnology, Biology and Medicine*, 2020, 26, 102178.
- [4] Iranpour Anaraki, Neda, et al., *Advanced Functional Materials*, 2022, 32.9, 2110253.

Yevheniia Kholina (1), Arkadiy Simonov (1)

[1] *ETH Zürich, Switzerland, Department of Materials, Laboratory for Multifunctional Ferroic Materials*

Prussian Blue analogues,  $M[M'(CN)_6]_{1-x} nH_2O$ , which we abbreviate here as  $M[M']$  ( $M$  and  $M'$ =transition metal ions), is a diverse family of cyanide materials, which is intensely investigated for its potential application for hydrogen storage, as catalysts and as electrode materials. Applications that require efficient mass transport utilize the ability of the structure to accommodate a large number of  $M'(CN)_6$  vacancies, which create a highly connected porous network. It was theoretically shown that the connectivity and the accessible volume of such a network depend on the local structure [1]. Therefore, to optimize mass transport properties not only the number of vacancies but also their distribution must be precisely controlled. In this work we show how to tune the local structure of  $Mn[Co]$  Prussian Blue analogues grown in gel by varying the crystallization parameters: the type of gel (Figure 1), the crystallization temperature, the concentration of reactants, and the concentration of chelating agents. We probe the defect distribution by single-crystal x-ray diffuse scattering, which allows quantitative characterization of the local structure. All of the above-mentioned parameters allow smooth continuous control of diffuse scattering and thus of the local order in  $Mn[Co]$  crystals.

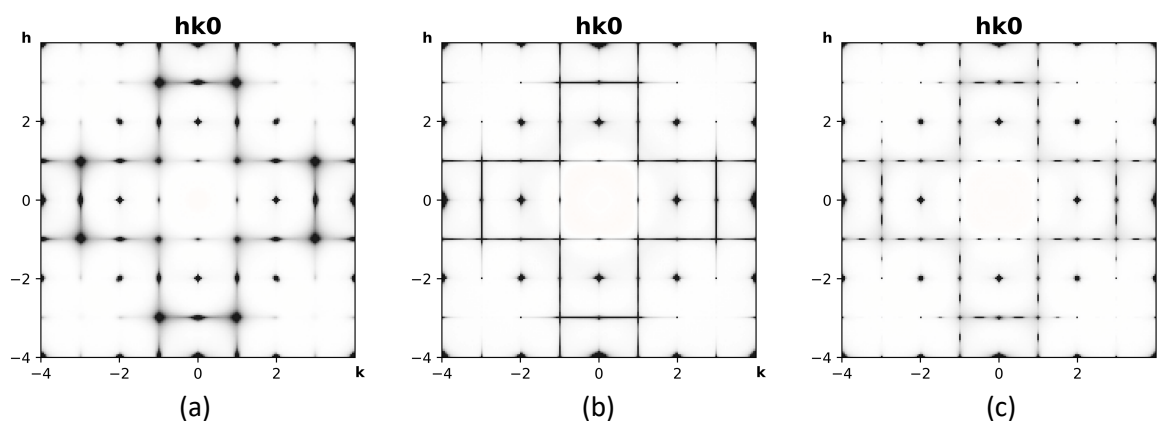


Figure 1 - The  $hk0$  slice of experimental diffuse scattering from  $Mn[Co]$  Prussian Blue Analogue, grown in three different gel media: agar gel (a), polyacrylamide gel (b) and silica gel (c).

[1] Simonov, Arkadiy, et al. "Hidden diversity of vacancy networks in Prussian blue analogues." *Nature* 578.7794 (2020): 256-260.

# Solid-state synthesis of cyclo Leu-Leu: zwitterionic form vs trifluoroacetic acid salt

Talk  
14

A. F. Perez Mellor (1), D. Rosa Gastaldo (1), X. Wang (1), N. Giamboni (1), C. Besnard (2), L. Guenee (2), M. Patigniez (2), J. Brazard (1), T. Adachi (1), T. Buergi (1)

(1) Department of Physical Chemistry, University of Geneva, Switzerland. (2) Laboratory of Crystallography, University of Geneva, Switzerland.

In this work we investigate the cyclization of linear Leu-Leu taking place in the solid-state upon heating [1]. In addition, the role of the chirality of the residue is also studied. Two different starting points, the zwitterionic species [2] (stabilized by water molecules) and the trifluoroacetic acid salt form are considered. Interestingly, the newly formed species (cyclo Leu-Leu), which belongs to the diketopiperazine family, has fascinating self-assembly properties due to the formation of a two-hydrogen bond pattern [3]. Several techniques, such as in-situ X-ray powder diffraction, optical microscopy, thermogravimetry analysis, and nuclear magnetic resonance, are combined to unravel all the processes that take place during the thermal reaction.

In summary, we have found that the thermodynamic properties of the thermal reaction are highly dependent on the starting point. In the case of the zwitterionic form, the thermal reaction happens in the solid state, while if the starting point is the TFA salt, the initial powder melts, and when the thermal reaction occurs, the crystals form. We identified a crystal growth stage in both cases by a ripening mechanism [4]. Figure 1 shows the different stages in both cases. Interestingly, if the cyclization occurs in the solid state, the system retains the initial absolute configuration distribution of the residues; otherwise, the racemization occurs.

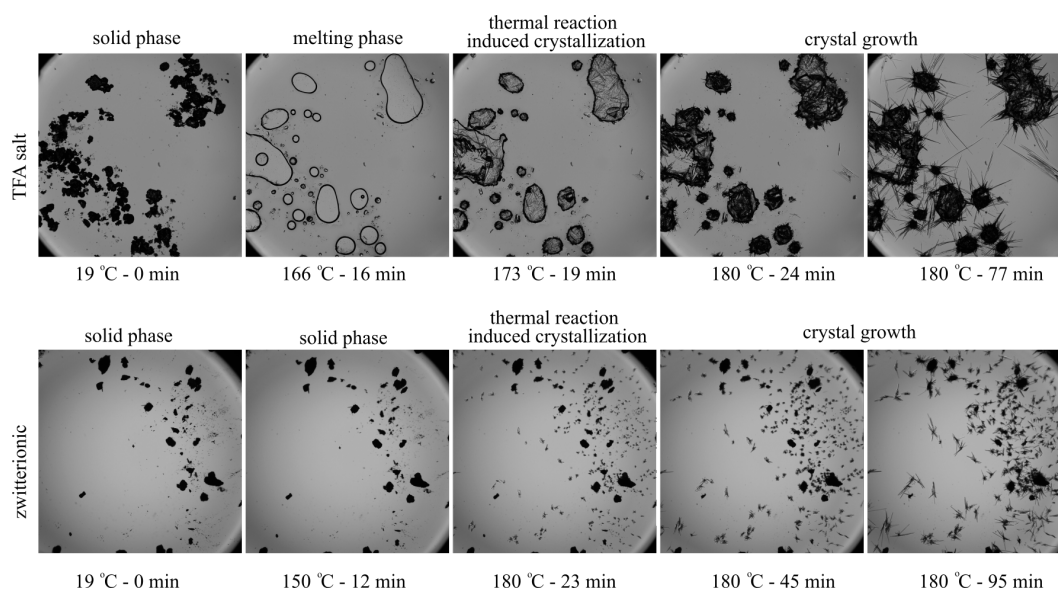


Figure 8- Optical images taken during the solid-state synthesis of cyclo (R)Leu-(S)Leu. The field of view is 4mm x 4mm.

[1] Marat A. Ziganshin, et al. J. Phys. Chem. B (2017).

[2] Gorbitz, et al. Chem. Eur. J. (2001): 5153-5159.

[3] Manchineella S, et al. Chempluschem (2017): 88-106.

[4] Ostwald, W. Zeitschrift für Physikalische Chemie. 22: 289–330 (1897).

## 2022 SGK-SSCr Meeting – Abstracts : III – Posters

# On the Cutting Edge of Electron Diffraction Quality

Poster  
1

Eric Hovestreydt (1), Johannes Merkelbach (1), Christian Jandl (1), Gunther Steinfeld (1), Danny Stam (1)

[1] ELDICO Scientific AG, PARK innovAARE, 5234 Villigen-PSI, Switzerland.

Electron diffraction (3D ED) has recently emerged as a powerful tool for structure determination on crystallites in the nanometer range, as it allows to bypass the common bottleneck of growing single crystals, big enough for x-ray diffraction. 3D-ED, using both the continuous rotation method and software as we know from X-ray crystallography, is gaining a lot of attention in all fields of research from organic and inorganic molecules, over polymorphism, geological sciences, natural products, biomolecules, material sciences to energy-storage materials and many others.

Here we showcase results from our electron diffractometer, the first entirely dedicated device for 3D ED, on representative case studies dealing with challenging organic compounds to demonstrate the benefits over TEM-based MicroED experiments. Pioneers in the field of electron diffraction already agree that a dedicated device is of great advantage for all fields of nano-crystallography.

As a benchmark and to show the capabilities of a dedicated electron diffractometer, we recently performed 3D ED experiments on Metaxalone,  $C_{12}H_{15}NO_3$ . Sold as Skelaxin, it is a muscle relaxant, but its exact mechanism of action is still not known. Metaxalone exhibits various polymorphic forms with substantial effects on e.g. solubility and bioavailability, one of which could only be obtained[1] as nanometer-sized needles and thus required electron diffraction for accurate structure elucidation.

The data quality obtained is clearly superior to previously reported[1], despite room-temperature data collection, indicating a higher performance of a dedicated diffractometer compared to equipment commonly used until today.

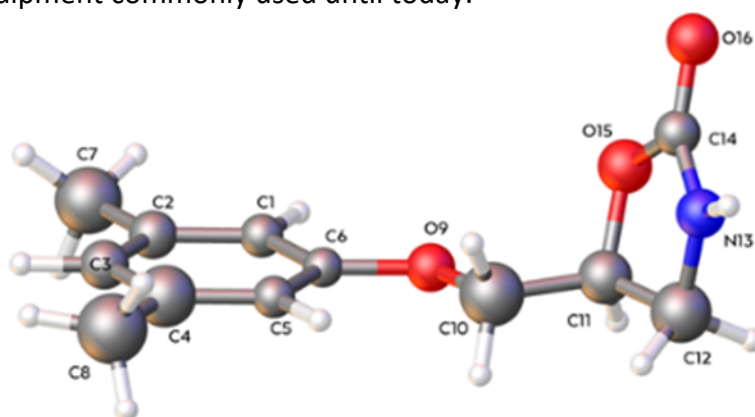


Figure 9- Metaxalone from nano-crystal.

The data quality obtained is clearly superior to previously reported[1], despite room-temperature data collection, indicating a higher performance of a dedicated diffractometer compared to equipment commonly used until today.

[1] V. Hamilton et al., *Cryst. Growth Des.*, 20, 7 (2020) 4731–4739

# Quantum crystallographic evaluation of S-C and P-C bonds in sulfur and phosphorus ylides

Poster  
2

Yaser Balmohammadi<sup>1</sup>, Lorraine A. Malaspina<sup>1</sup>, Simon Grabowsky<sup>1</sup>

<sup>1</sup>Department of Chemistry, Biochemistry and Pharmaceutical Sciences, University of Bern, Switzerland

An ylide compound is a neutral molecule containing a formal double bond for which actually the charge-separated resonance form has a high stabilizing contribution (see Figure 1a). The negative charge is usually located at a carbon atom connected to a heteroatom with a formal positive charge (usually nitrogen, phosphorus or sulfur). This charge distribution has direct consequences on the reactivity of ylides leading to a lot of applications in organic synthesis as reagents or reactive intermediates. Phosphorus ylides or phosphonium ylides have been widely used in organometallic and organic synthesis, most famously as Wittig reagents in the Wittig reaction.<sup>i</sup> Sulfur ylides (sulfonium ylides and sulfoxonium ylides) are also employed in organic synthesis, e.g. in the Johnson–Corey–Chaykovsky reaction.<sup>ii</sup>

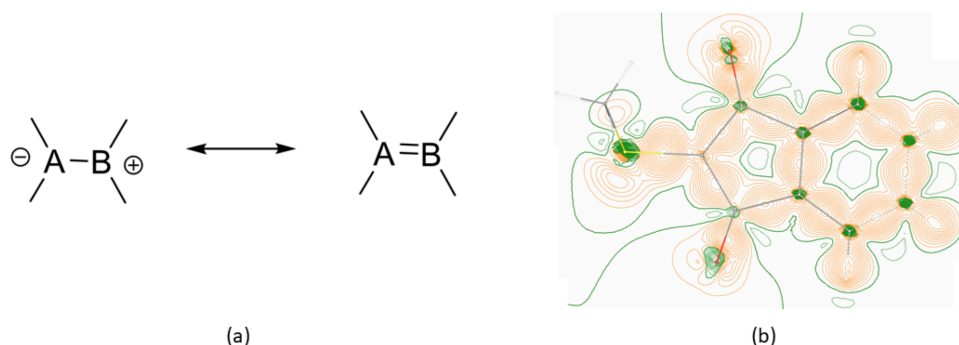


**Figure 1.** (a) two resonance forms of an ylide compound, (b) 2-D deformation density map of sulfur ylide compound

For those reasons, ylides are textbook examples for the interplay between Lewis resonance forms and molecular reactivity/ function. Hence, a full complementary bonding analysis<sup>iii</sup> revealing the nature and character of the P-C and S-C bonds in ylides in detail is of practical importances and will also clarify concepts such as hypervalency of P and S atoms as well as the interplay between covalency and ionicity of heteroatom bonds. To the best of our knowledge, there are four experimental charge density studies about these bonds using multipole refinement<sup>iv v</sup>, and there is no Hirshfeld atom refinement (HAR) and X-ray wavefunction (XCW) fitting study about these bonds. In this study, our aim is to perform full X-ray wavefunction refinements (HAR + XCW fitting)<sup>vi</sup> plus complementary bonding analyses to evaluate the C-S and C-P bonds in two ylide compounds measured at 100K with Ag K $\alpha$  radiation to high resolution (Figure 1b).

<sup>i</sup> Johnson AW (1993) Ylides and imines of phosphorus. Wiley, New York

<sup>ii</sup> Weber L (1983) Angew. Chem Int Ed Engl 22:516–528

<sup>iii</sup> Grabowsky, Simon, ed. Complementary Bonding Analysis. Walter de Gruyter GmbH & Co KG, 2021.

<sup>iv</sup> Deuerlein, Stephan, et al. Organometallics 27.10 (2008): 2306-2315.

<sup>v</sup> Ahmed, Maqsood, et al. The Journal of Physical Chemistry A 117.51 (2013): 14267-14275.

<sup>vi</sup> Woińska, Magdalena, et al. ChemPhysChem 18.23 (2017): 3334-3351.

# Structure Determination of Nanocrystalline MOFs Using Electron Diffraction

Poster  
3

Christian Jandl (1), Johannes Merkelbach (1), Gunther Steinfeld (1), Eric Hovestreydt (1)

[1] ELDICO Scientific AG, Villigen, Switzerland.

Electron diffraction (3D-ED, MicroED) is gaining more and more momentum as a technique for the structural elucidation of challenging compounds as it bypasses the main limitation of growing crystals of suitable size for single-crystal X-ray diffraction. As such it has already found applications in various fields of research from organic and inorganic compounds, over pharmacology, natural products, geological sciences, biomolecules, materials science to energy-storage materials and others.

As porous materials commonly obtained from solvothermal synthesis MOFs often pose a challenge for traditional X-ray crystallography as their inherent properties do not allow for recrystallisation, which makes structural analysis dependent on obtaining suitable single crystals straight from the synthesis. Being able to use nanocrystalline (“as synthesised”) material makes electron diffraction the perfect tool to tackle this problem and determine structures from crystals that are too small even for synchrotron facilities.

We show a range of examples measured on the ELDICO ED-1 electron diffractometer demonstrating the potential of 3D-ED for applications in the field of porous coordination compounds and benefits of a dedicated electron diffractometer.

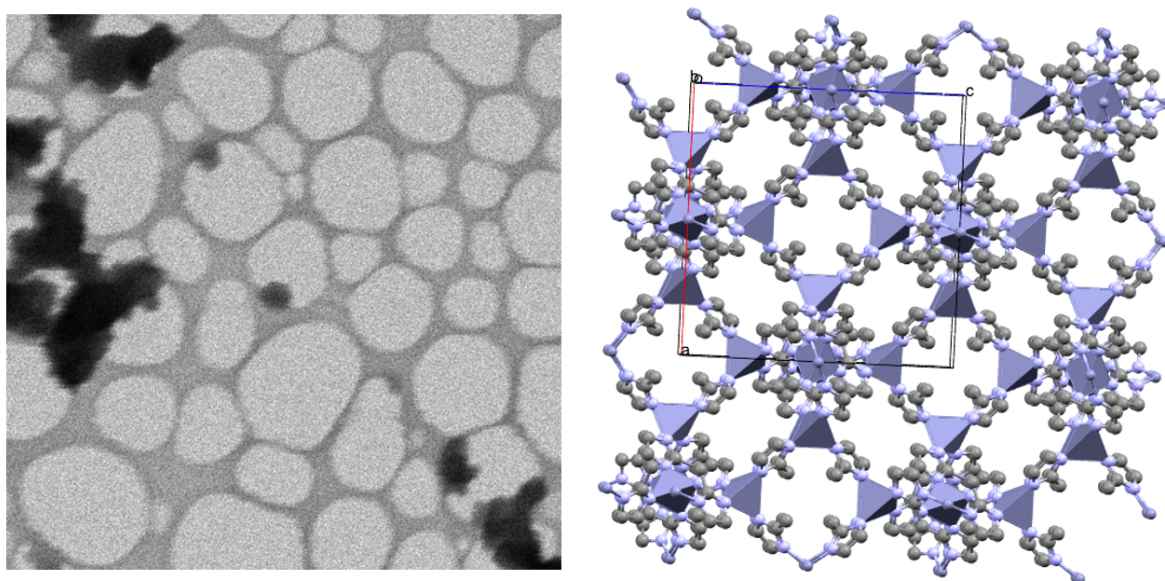


Figure 10 – Left: STEM (scanning transmission electron microscopy) image of a nanocrystalline ZIF-8 sample, field of view 10x10  $\mu\text{m}$ . Right: Packing diagram of the crystal structure obtained from the respective sample.

## Scattering methods to find weaknesses in enveloped viruses

Samuel Watts (1), Eliane Hänni (1), Stefan Salentinig (1)

Poster

4

[1] Chemistry Departement, University of Fribourg – 1700 Fribourg, Switzerland.

Enveloped viruses, such as influenza, SARS CoV-2, Ebola and HIV, are highly problematic pathogens that have a great toll on human society.[1] These viruses are characterized by an outer lipid layer (lipid envelop) in which the proteins for host-cell recognition and attachment are imbedded and an inner core (nucleocapsid) containing the genetic information for replication protected by a protein shell.[2] This work aims at understanding how amphiphiles molecules interact with a model enveloped viruses (phi6) on a nano-structural level, using a combination of scattering and spectroscopic methods. Ethanol and the antimicrobial peptide LL-37 (from the human immune system) were chosen as amphiphilic molecules. The first for its common use as disinfectant, the second as a potential antiviral drug.

Small angle X-ray scattering allowed to investigate *in situ* the structural changes. Ethanol induced mainly structural modifications in the lipid envelope, which was separated for the rest of the particle and transition from a bilayer like structure to a sponge phase. Similarly, LL37 was shown to integrate to the bilayer and led to separation envelope -nucleocapsid separation.

The link between the lipid layer and the nucleocapsid was highlighted as the Achilles heel of enveloped viruses. This structural understanding may be useful when designing new broad-spectrum antiviral drugs.

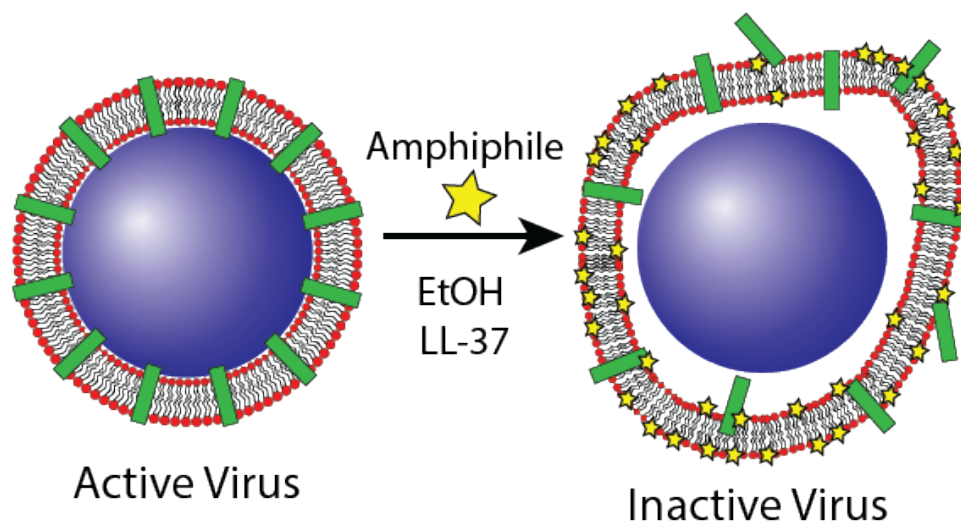


Figure 11- Schematic for the structural modification of enveloped viruses by Ethanol and LL37

[1] Parvez, M. K.; Parveen, S. *Intervirolgy* 60 (2017), 60, 1-7

[2] Ryu, W.-S., Chapter 2 - Virus Structure. In *Molecular Virology of Human Pathogenic Viruses*, Ryu, W.-S., Ed. Academic Press: Boston, 2017; pp 21-29.

# Identification of reduced-symmetry palladium-based metal-supramolecular assemblies

Poster  
5

Sylvain Sudan (1), Ru-Jin Li (1), Suzanne Jansze (1), Farzaneh Fadaei-Tirani (1), Rosario Scopelliti (1), André Platzek (2), Robin Rudolf (2), Kristina Ebbert (2), Guido Clever (2) and Kay Severin (1)

[1] Institut des Sciences et Ingénierie Chimiques, Ecole Polytechnique Fédérale de Lausanne (EPFL), 1015 Lausanne, Switzerland. E-mail: sylvain.sudan@epfl.ch. [2] Fakultät für Chemie und Chemische Biologie, Technische Universität Dortmund, 44227 Dortmund, Germany.

Palladium-based assemblies have been widely studied and applied to catalysis or medicinal chemistry owing to their versatile host-guest chemistry. Heteroleptic assemblies increase their structural complexity and help mimic biological systems. Crystallography is a powerful tool for determining chemical reaction-mechanisms in supramolecular cages of which the crystallisation yields crystals containing plenty of solvent molecules in the cavities. This solvent may leave the crystal during the preparation and mounting, causing numerous problems, such as partial counter-ions and solvents, which are painstaking to model and lead to precarious reflection/parameter ratios. Diffraction from such crystals is often weak and limited ( $\geq 1 \text{ \AA}$ ), and obtaining even a rough structure is considered a big success and the result of hard work and perseverance in solving and refining the structure. In the end, even a rough structure is precious and revealing to chemists.

A selection process yielded a novel hexanuclear palladium-based assembly, comprising two different dipyriddy ligands, of the formula  $[\text{Pd}_6(\text{L1})_6(\text{L2})_6](\text{BF}_4)_{12}$  (**1**, **Figure 1a**); this was the stablest member of a virtual combinatorial library of  $[\text{Pd}_n\text{L}_{2n}](\text{BF}_4)_{2n}$  complexes.<sup>[1]</sup> Adding  $\text{Li}^+$ , as a guest, to one of the complexes resulted in converting the starting  $\text{Pd}_2\text{L}_4$  species to a low-symmetry  $\text{Pd}_4\text{L}_8$  structure (**2**, **Figure 1b**), encapsulating two solvated  $\text{LiBF}_4$  ion pairs. Structural analysis showed different intramolecular interactions to be similar to those in natural and synthetic foldamers and the possibility of structural complexity for homoleptic  $\text{Pd}_n\text{L}_{2n}$  systems.<sup>[2]</sup>

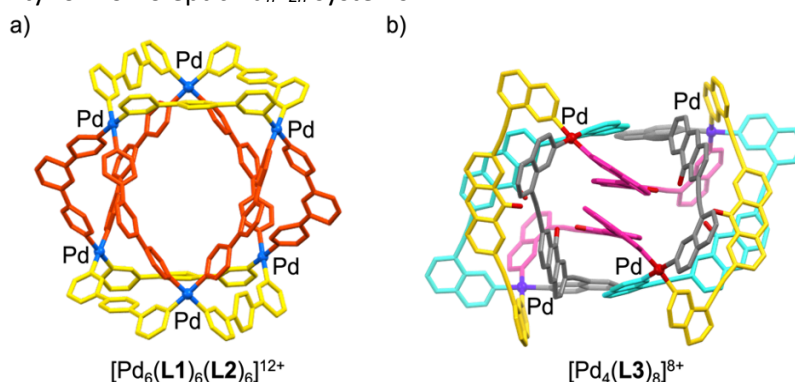


Figure 12- Graphical representations of the molecular structures of  $[\text{Pd}_6(\text{L1})_6(\text{L2})_6]^{12+}$  (a) and of  $[\text{Pd}_4(\text{L3})_8]^{8+}$  (b) in the crystal. The colours indicate the different ligands (a), symmetry-related ligands, and  $\text{Pd}^{2+}$  ions (b).

Compounds **1** and **2** are lucky examples of such assemblies. Indeed, their resolution is high enough (0.81  $\text{ \AA}$  for **1**, 0.84 for **2**), their intensities, too ( $R_\sigma = 0.068$  for **1**, 0.021 for **2**) and  $R_{\text{int}}$  quite respectable (0.051 for **1**, 0.044 for **2**). Nevertheless, a satisfactory refinement ( $R_1 = 0.074$  for **1** and 0.084 for **2**) could only be reached by imposing somewhat questionable RIGU and SIMU restraints (**2**) or very exacting RIGU 0.001 (**1**) for all atoms. Finally, in **1**, as many as 9  $\text{BF}_4^-$  and 65 ACN, had to be removed from the model with the help of a solvent mask in Olex2<sup>[3]</sup>, and 8 and 27 in **2**.

[1] Sudan, S.; Li, R.-J.; Jansze, S. M.; Platzek, A.; Rudolf, R.; Clever, G. H.; Fadaei-Tirani, F.; Scopelliti, R.; Severin, K. *J. Am. Chem. Soc.* **2021**, *143*, 1773–1778

[2] S. Sudan, F. Fadaei-Tirani, R. Scopelliti, K. E. Ebbert, G. H. Clever, K. Severin, *Angew. Chem. Int. Ed.* **2022**, DOI : doi.org/10.1002/anie.202201823

[3] O.V. Dolomanov and L.J. Bourhis and R.J. Gildea and J.A.K. Howard and H. Puschmann, *Olex2: A complete structure solution, refinement and analysis program*, *J. Appl. Cryst.*, (2009), **42**, 339-341.

# Synthesis and structural determination by X-Ray crystallography of metal nanoclusters

Poster  
6

Khadijetou Ahmed Ethmane (1), Thomas Bürgi (1), Céline Besnard (1), Arnulf Rosspeintner (1)

[1] Faculty of Science, University of Geneva – 1205 Geneva, Switzerland.

Noble metal nanoclusters are a special class of nanomaterials with sizes varying between 1 and 3 nm which exhibit very peculiar molecule-like properties. These properties make them promising candidates for various applications including in catalysis, bioimaging or sensing [1]. These nanoclusters are atomically precise with a number of metallic atoms ranging from around 10 to a few hundreds and are protected by a shell of organic ligands [1].

Determining the exact structure of these compounds is essential to a good understanding their properties and such structure determination can be achieved by X-Ray crystallography. To investigate the structure-size relationship and the evolution of the structure with the size of nanomaterials, new nanoclusters were synthesised and crystallised. A detailed analysis of their structures was conducted after X-Ray diffraction and some spectroscopic properties were measured. The new clusters are chiral. Interestingly, the chirality of the  $\text{Ag}_{21}\text{Au}_8$  alloy cluster arises from the helical arrangement of the gold atoms.

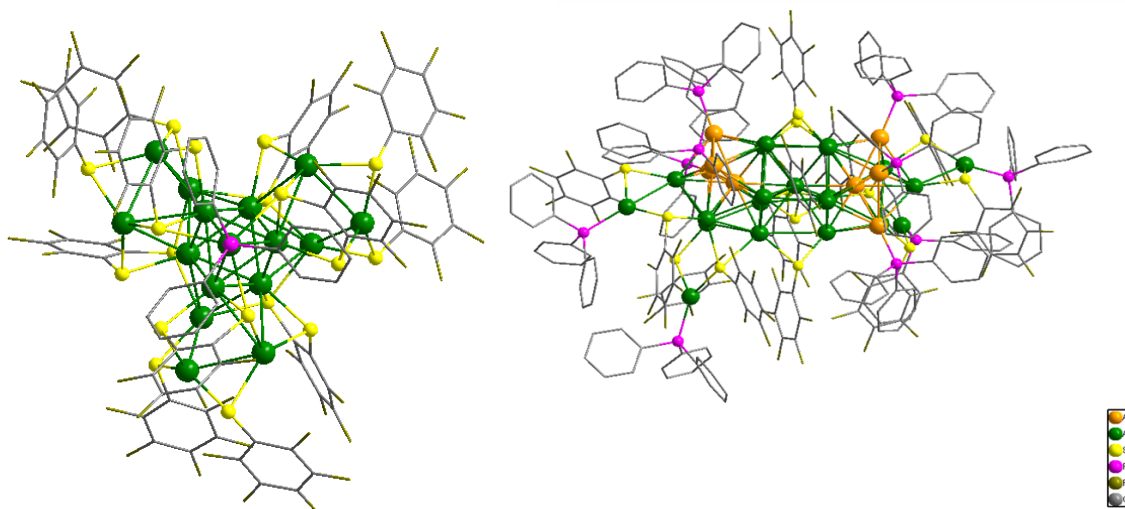


Figure 13- Crystal structures of  $\text{Ag}_{16}$  (left) and  $\text{Ag}_{21}\text{Au}_8$  (right) clusters. Color legend: green, Ag; orange, Au; yellow, S; pink, P; grey, C; dark gold, F.

[1] Meng Zhou, Chenjie Zeng, Yuxiang Chen, Shuo Zhao, Matthew Y.Sfeir, Manzhou Zhu, Rongchao Jin. Nature Communications 7 (2016): 13240

## Unblocking Ion-occluded Pore Channels in Poly(triazine imide) Framework

Poster  
7

Heng-Yu Chi (1), Cailing Chen (2), Kangning Zhao (1), Luis Francisco Villalobos (1), Pascal Alexander Schouwink (3), Laura Piveteau (4), Kenneth Paul Marshall (5), Qi Liu (1), Yu Han (2),\* and Kumar Varoon Agrawal (1)\*

[1] Laboratory of Advanced Separations (LAS), École Polytechnique Fédérale de Lausanne (EPFL), 1950 Sion, Switzerland. [2] Advanced Membranes and Porous Materials Center, Physical Sciences and Engineering Division, King Abdullah University of Science and Technology, Thuwal 23955, Saudi Arabia. [3] Institute of Chemical Sciences and Engineering (ISIC), École Polytechnique Fédérale de Lausanne (EPFL), 1950 Sion, Switzerland. [4] Institute of Chemical Sciences and Engineering, NMR Platform, École Polytechnique Fédérale de Lausanne (EPFL), 1015 Lausanne, Switzerland. [5] Swiss-Norwegian Beamlines, European Synchrotron Radiation Facility, 38000 Grenoble, France.

Two-dimensional (2D) crystalline, nanoporous materials have attracted significant attention in important applications such as molecular separation and catalysis. Nanoporous poly(triazine imide) (PTI), belonging to the family of graphitic carbon nitrides, is composed of imide-bridging of triazine rings intercalated with metal halides through the ionothermal synthesis. PTI hosts high density ( $1.6 \times 10^{14} \text{ cm}^{-2}$ ) of 3.4 Å-sized nanopores with outstanding chemical and thermal stability attractive for developing high-performance gas separation membrane [1]. However, the main challenge for the separation applications is that the intercalated ions block the desired molecule transport channels. Thus, removal of the intercalated ions is crucial to access the porous framework of PTI.

The determination of the precise structure of PTI is hampered by the fact that C, N,  $\text{Li}^+$ , and  $\text{H}^+$  are poor X-ray scatterers and become further complicated by the small lateral size and the occurring structural disorder. In addition, the possible layer displacement of PTI after depletion of ions from AA' stacking to AB stacking [2], resulting in the pore occlusion by the triazine ring in the adjacent layer; however, so far, there has not been conclusive evidence to identify the atom position. Herein, we demonstrate the facile approach to tune the concentration of intercalated  $\text{Li}^+$  and  $\text{Cl}^-$  ions in PTI framework using acid treatment while preserving the crystallinity and the morphology of PTI nanosheets. The direct visualization of ion-depleted PTI using integrated differential phase-contrast scanning transmission electron microscopy (iDPC-STEM) fueled by X-ray scattering techniques and solid-state nuclear magnetic resonance spectroscopy confirms the coexistence of open channels and occluded domains for the first time. The extent of open channels with AA' stacks increases with higher depletion level. An increasing population of open channels vastly improves the proton conductance through PTI from 1.1 mS/cm to 5.4 mS/cm, giving a prospect of PTI for application in molecular transport.

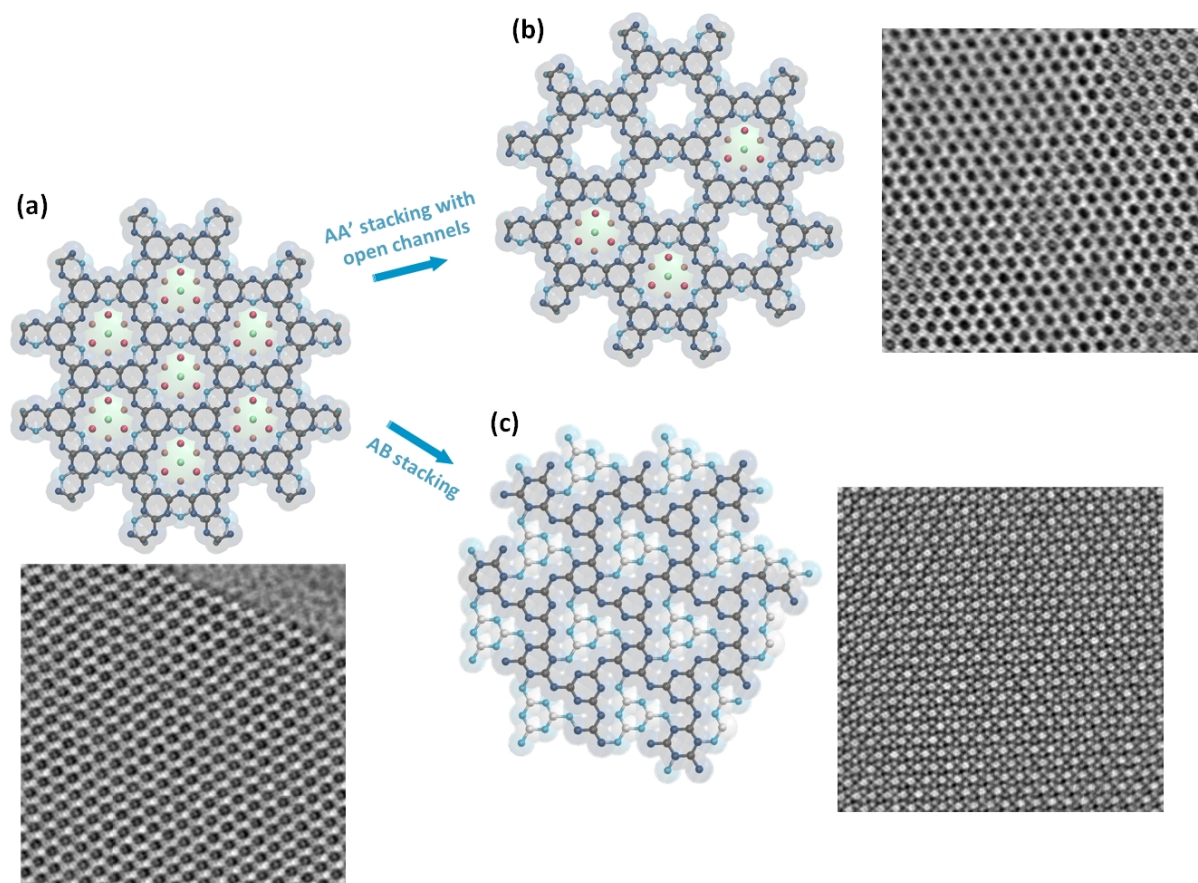


**Figure 14-** Schematic representation of three different PTI structural models and corresponding iDPC-STEM images: (a) as-synthesized PTI (AA' stacks), (b) PTI with partial ion occlusion with open channels (AA' stacks), and (c) PTI with AB stacks without intercalated ions.

[1] Villalobos L. F., Vahdat M. T., Dakhchoune M., Nadizadeh Z., Mensi M., Oveisi E., Campi D., Marzari N., Agrawal K. V., *Sci. Adv.*, 6 (2020): eaay9851.

[2] Suter T. M., Miller T. S., Cockcroft J. K., Aliev A. E., Wilding M. C., Sella A., Cora F., Howard C. A., McMillan P. F., *Chem. Sci.*, 10 (2019): 2519-2528.

# Discovery and characterization of a new aluminium phosphate sulfate mineral

Poster  
8

Gwilherm Nénert(1), Thomas Witzke(1)

[1] Malvern Panalytical B. V., Almelo, The Netherlands.

A new mineral with the composition  $\text{Al}_2(\text{PO}_4)(\text{SO}_4)(\text{OH},\text{F})(\text{H}_2\text{O})\cdot 6\text{H}_2\text{O}$  was found on the dump of the Lichtenberg open cast, Ronneburg, Thuringia, Germany. In the open cast and surrounding mines uranium-bearing alumn shale was mined from 1950's to 1990's. The Ronneburg mining area was one of the largest uranium producers in Europe. The new mineral is an alteration product and was formed on the mine dump. It forms white aggregates of irregular intergrown, tiny acicular crystals of less than 0.1 mm in length and was found only in very small amounts. Lattice parameter and crystal structure were determined from powder diffraction data. This new mineral exhibits  $P-1$  symmetry and lattice parameters  $a=6.129 \text{ \AA}$ ,  $b=9.856 \text{ \AA}$ ,  $c=11.433 \text{ \AA}$ ,  $\alpha=70.284^\circ$ ,  $\beta=85.84^\circ$ ,  $\gamma=82.557^\circ$  and  $V = 644.36 \text{ \AA}^3$ . For  $Z = 2$ , the calculated density is  $2.09 \text{ g/cm}^3$ . It is structurally related to sanjuanite,  $\text{Al}_2(\text{PO}_4)(\text{SO}_4)(\text{OH})\cdot 9\text{H}_2\text{O}$ , and arangasite,  $\text{Al}_2(\text{PO}_4)(\text{SO}_4)\text{F}\cdot 9\text{H}_2\text{O}$ . It displays a layered structure of chains of  $\text{AlO}_6$  octahedra and  $\text{PO}_4$  tetrahedra. These units forming channels parallel to the  $a$  axis. The  $\text{SO}_4$  tetrahedra are situated close to the chains but probably linked to it only by hydrogen bonds. There are 6 molecules of crystallization water and one water molecule per formula unit is occupying the channels in the structure. Very similar aluminophosphate chains were found in sanjuanite (Colombo *et al.*, 2011).

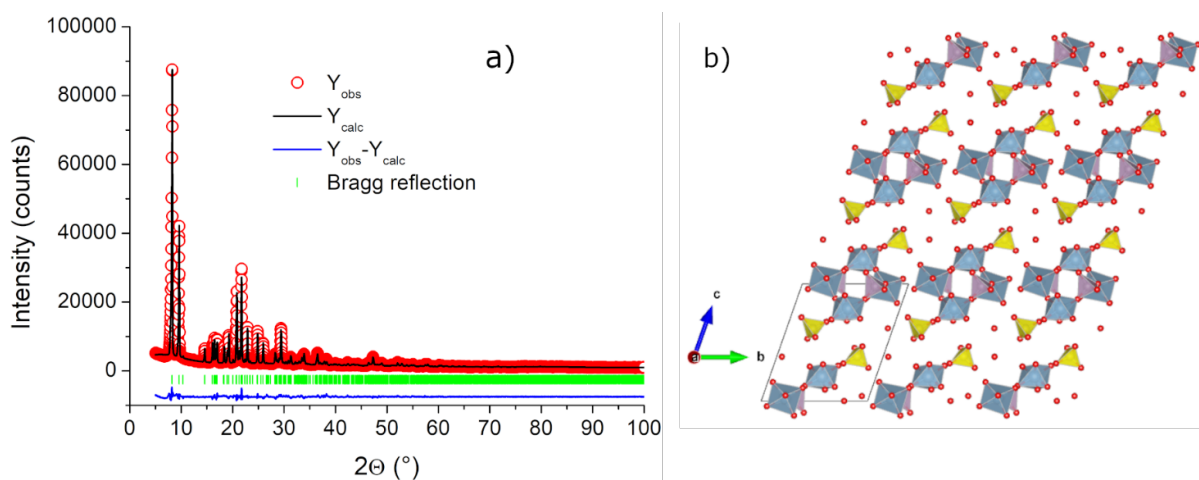


Figure 15- a) Rietveld refinement of  $\text{Al}_2(\text{PO}_4)(\text{SO}_4)(\text{OH},\text{F})(\text{H}_2\text{O})\cdot 6\text{H}_2\text{O}$  ( $R_{wp} = 5.3\%$ ) and b) the corresponding crystal structure projected along the  $a$  axis.

[1] Colombo, F., Rius, J., Pannunzio-Miner, E.V., Pedregosa, J.C., Camí, G.E., Carbonio, R.E. (2011) *The Canadian Mineralogist*: 49: 835-847.

# Investigation and characterization of new polymorphic forms of the API Na-naproxen from powder diffraction data

Poster  
9

Maria Orlova (1), Gwilherm Nénert (2)

[1] Malvern Panalytical B. V. Switzerland Branch, Volketswil, Switzerland.

[2] Malvern Panalytical B. V., Almelo, The Netherlands.

Sodium naproxen is widely used as a non-steroidal anti-inflammatory active pharmaceutical ingredient (API). The crystal structure of this API has been reported back in 1990 [1]. Despite 3 decades of research on this API, only one single polymorph has been reported. On the other hand, physicochemical stability may become a serious problem during new drug development and thus pseudo-polymorphism have been widely investigated for sodium naproxen. So far, 4 hydrates have been reported and characterized [2]. So, while the pseudo-polymorphism is rather rich, polymorphism is unusually simple with only one known representative. This is a rather unusual case as polymorphism for APIs tends to be rather rich [3]. With that in mind, we have started re-investigating sodium naproxen. In this contribution, we are reporting evidence for 2 new polymorphs of sodium naproxen. One of these new polymorphs has been fully characterized structurally from powder diffraction data. Its crystal structure is very similar to previously reported structure with only the methoxy group orientation is changed. We are presenting in Figure 1, the comparison between the 2 polymorphs. This contribution calls for a necessary re-investigation of this widely used API.

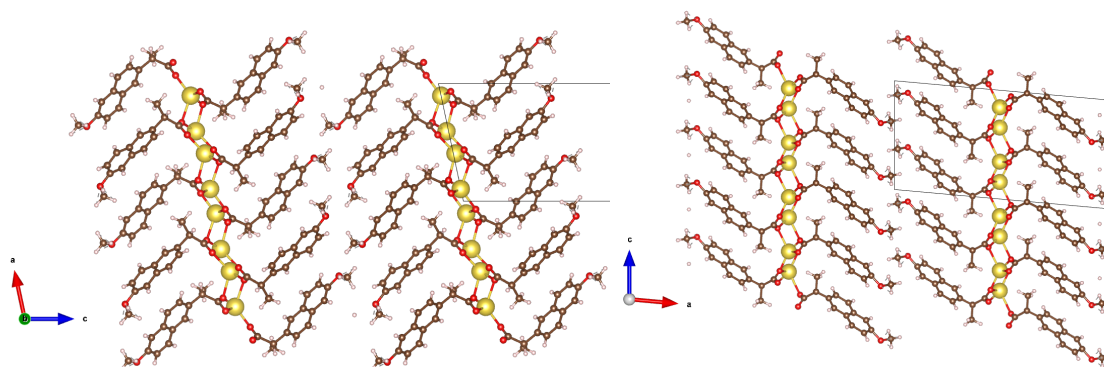


Figure 16- (Left) Known polymorph of sodium naproxen [1] and comparison with the (right) newly characterized polymorph.

[1] Kim, Y. B.; Park, I Y; Lah, W R *Arch. Pharm. Res.*, **1990**, *13*(2), 166 – 173.

[2] Bond, A. D.; Cornett, C.; Larsen, F. H.; Qu, H.; Rajjada, D.; Rantanen, J. *IUCrJ*, **2014**, *1*, 328 – 337.

[3] Lee, E. H. *Asian Journal of Pharmaceutical Sciences*, **2014**, *9*, 163 – 175.

## The benefits of Cu K $\beta$ radiation for the structure determination of crystalline sponges

Florian Meurer(1), Carolina von Essen(2), Clemens Kühn(2), Horst Puschmann(3) and Michael Bodensteiner(1)

(1) Universität Regensburg, Universitätsstr. 51, Germany, (2) Merck Innovation Center, Merck KGaA, Frankfurter Str. 250, Darmstadt, Germany, (3) OlexSys Ltd, Durham University, DH1 3LE, UK

The Crystalline Sponge method enables the structural elucidation of scarce, small organic analytes and hard-to-crystallize compounds. By the diffusion of solvent and analyte molecules into the cavities of a metal-organic framework (the crystalline ‘sponge’) and molecular orientation by the MOF’s functional groups, an analyte becomes part of the crystal structure and thus observable through X-ray diffraction methods.[1]

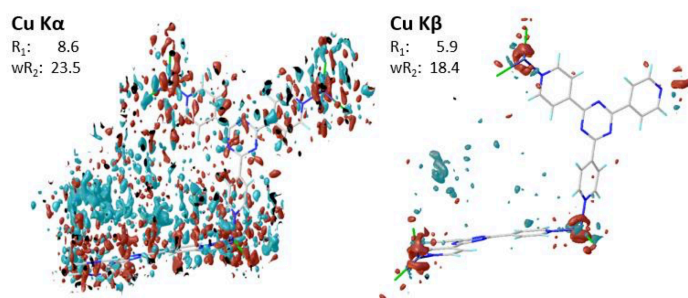


Figure 1: Comparison residual electron density maps with the different wavelengths (iso-level:  $0.4 \text{ e}^{-\text{Å}^{-3}}$ )

Problems inherent to the structural elucidation of MOFs limit the possibilities of this method. These include weak host-guest interaction, incomplete diffusion, twinning, disorder of both analyte and solvent, and sample decay. As much as the physical and chemical aspects of the method have recently been improved, the crystallographic aspects pose challenging problems for the method. As we have recently adopted the use of the very rarely used Cu K $\beta$  radiation in our X-ray department and found promising results in the analysis of our small molecule data, we also applied Cu K $\beta$  radiation to the Crystal sponge method and compared it to the more commonly used wavelength Cu K $\alpha$  in a total of six comparison experiments. Cu K $\beta$  inherits a shorter wavelength than Cu K $\alpha$  radiation ( $1.39222 \text{ \AA}$  compared to  $1.54187 \text{ \AA}$ ) and thus results in up to 38 % more unique reflections. This is mainly due to the maximum resolution of  $0.72 \text{ \AA}$  is accessible for Cu K $\beta$  radiation, compared to  $0.80 \text{ \AA}$  for Cu K $\alpha$  radiation. Less absorption by consistently 25 % in absorption coefficient for Cu K $\beta$  leads to less background and radiation damage.[2]

This results in better crystallographic models for the Cu K $\beta$  data sets: Significantly lower quality parameters were obtained in every Cu K $\beta$  experiment. Bond precision was mainly better and the compared residual electron density maps (Fig. 1) look much cleaner. Additionally, more solvent positions could be modeled in the Cu K $\beta$  data sets. In total, way fewer restraints and no constraints had to be used in the models collected using Cu K $\beta$  radiation. Our findings suggest routine use of Cu K $\beta$  radiation – not only for the crystalline sponge method. The same advantages are to be expected in general for the structural elucidations of metal-organic frameworks but also standard small molecule crystallography.

[1] Hoshino, M., Khutia, A., Xing, H., Inokuma, Y. & Fujita, M. (2016). *IUCrJ*, **3**, 139–151.

[2] Meurer, F., von Essen, C., Kühn, C., Puschmann, H. & Bodensteiner, M. (2022). *IUCrJ* **9**, 5.

## Treatment of core electrons in Quantum Crystallography

Florian Kleemiss (1), Norbert Peyrerimhoff (2), Michael Bodensteiner(1)

(1) University of Regensburg, Universitätsstr 31, Regensburg 93053, Germany, (2) Durham University, Durham DH1 3LE, United Kingdom.

While the greatest advantage of Quantum Crystallography is undoubtedly the correct description of chemical bonding and electron density redistributions in the valence of atoms[1-3] the atomic core has slowly disappeared from the focus of method developers and researchers.

Despite recent advances in automation and the availability of non-spherical scattering factors, the high residual density around heavy scatterers, especially in high-resolution data sets, still cannot be explained. It remains an open discussion what the source of these artifacts is. In the proposed presentation, it will be demonstrated that two effects caused by core electrons could explain the observed patterns: The assumption of forward scattering in resonant scattering treatment (a.k.a. anomalous diffraction)[4] could be a significant overestimation for high angle diffraction data. Additionally, the missing cusp in Gaussian functions which are frequently used to describe the atomic density compared to Slater-type densities, which one would expect for atomic densities, might be a source for similar errors. In combination with the *also* Gaussian description of the atomic displacement, this yields insufficient Fourier behaviour for the description of the structure factors of heavy elements at high resolution. The effects on the calculated electron density around d-block atoms are visualized in Figure 1.

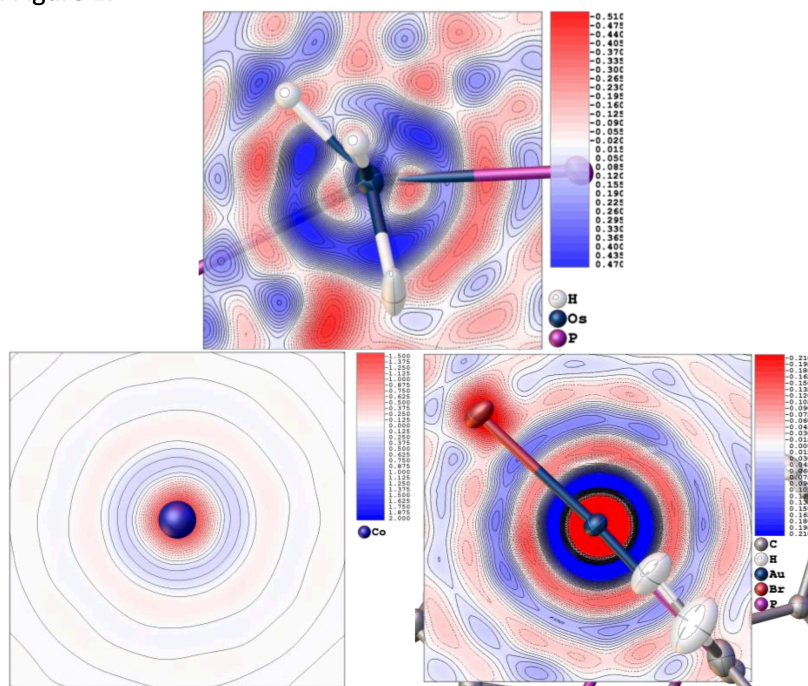


Figure 1 – Residual density after HAR of Os-hexy-hydride containing compound (top), difference density between newly proposed angular dependent treatment of resonant scattering correction  $f'$  and  $f''$  and classical treatment (bottom, left) and non-spherical refinement using Slater-type core density and all-electron treatment (bottom, right).

[1] Magdalena Woźńska et al. Chem. Phys. Chem. 18(23) (2017): 3334-3351.

[2] Simon Grabowsky et al. Chemical Science 8 (2017): 4159-4176.

[3] Alessandro Genoni, Piero Macchi, Crystals 10(6) (2020): 473.

[4] D. C. Creagh International Tables of Crystallography, Volume C (2016), 241-258.

Matteo Frigerio (1), Stefan Salentinig (1)

[1] Department of Chemistry, University of Fribourg, Chemin Du Musée 9, 1700 Fribourg, Switzerland

Oil/water interfaces are regions of excess free energy ubiquitous in colloids. The energy required for emulsification of oil in water is proportional to the interfacial tension. Certain ions were found to reduce the surface tension in a surfactant-free way<sup>1</sup>. This can help to reduce the consumption of surfactants while ensuring the decrease in surface tension and costs associated to the emulsification process from a practical point of view. However, the role of ions and the enhancement in interfacial features is still matter of debate as there are many factors, such as the polarizability<sup>2</sup> that come into play. Here we show that phosphate buffer, a commonly used buffer system in many studies, can significantly alter the lipid-water under certain pH conditions. Spinning drop tensiometry demonstrated the pH-triggered reduction of the interfacial tension between oil and water in presence of phosphate buffer. Monohydrogen phosphate (MHP) even appeared to crystallise at the water-triolein interface (Figure 1), in contrast to a plethora of other ions that were studied. Ellipsometry and Brewster angle microscopy showed the MHP triggered formation of layers at the interface, with a refractive index that is comparable to supersaturation conditions of the MHP. Moreover, stabilizer-free GMO cubosomes are used as a platform to analyse the integrations of the ions into lipid-water interfaces. Small angle X-ray scattering showed their structural transformation from double diamond Pn3m-type cubic phase in water<sup>3</sup> to primitive Im3m-type upon addition of MHP. Complementary techniques such as molecular dynamics and interfacial tension measurements all point in the same direction. Our results pave the way for a more systematic study on the interfacial role of ions in processes of biological relevance<sup>4</sup> such as calcium removal of long chain fatty acids from oil/water interface in lipid digestion.

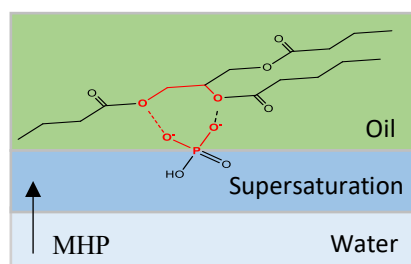


Figure 17. Sketch diagram for supersaturation conditions established upon MHP adsorption at the interface and following crystallization.

[1] Badizad, Mohammad Hasan, et al. "How do ions contribute to brine-hydrophobic hydrocarbon Interfaces? An in silico study." *Journal of Colloid and Interface Science* 575 (2020): 337-346.

[2] Chang, Tsun-Mei, and Liem X. Dang. "Recent advances in molecular simulations of ion solvation at liquid interfaces." *Chemical Reviews* 106.4 (2006): 1305-1322.

[3] Zabara, Mahsa, et al. "Multifunctional nano-biointerfaces: cytocompatible antimicrobial nanocarriers from stabilizer-Free cubosomes." *Advanced Functional Materials* 29.35 (2019): 1904007.

[4] Salentinig, Stefan, et al. "Transitions in the internal structure of lipid droplets during fat digestion ." *Soft Matter* 7.2 (2011): 650-661.

Poster

**Analysis of the structural dynamics in a NaNO<sub>3</sub>-promoted MgO-based CO<sub>2</sub>-sorbent during cyclic operation: an *in situ* time-resolved X-ray powder diffraction study**

Margarita Rekhtina, Maximilian Krödel, Felix Donat, Paula M. Abdala and Christoph R. Müller

*Laboratory of Energy Science and Engineering, Department of Mechanical and Process Engineering, ETH Zürich, Leonhardstrasse 21, 8092 Zürich, Switzerland.*

Carbon capture utilization and storage (CCUS) is a key technology to mitigate climate change by capturing CO<sub>2</sub> from large industrial sources and storing it underground, or by converting it further. CCUS processes rely on the availability of efficient CO<sub>2</sub> sorbents. In this regard, MgO-based materials are promising CO<sub>2</sub> sorbents due to their high theoretical gravimetric CO<sub>2</sub> capacity (1.09 g CO<sub>2</sub> per g MgO, MgO+CO<sub>2</sub>→MgCO<sub>3</sub>), high abundance, and environmental benignity.[1] Moreover, MgO-based sorbents operate in a temperature range of 200–450 °C which makes them suitable for hot flue gas streams. However, due to kinetic limitations, MgO requires the use of promoters – typically alkali metal nitrates which are molten under operational conditions. Currently, there is very active research aiming to advance these materials by improving their CO<sub>2</sub> uptake rates and cyclic stability. [2,3] However, there is still a limited understanding of the underlying structure-performance relationship that are, however, required for a rational advancement of the design of this class of sorbents. [4]

In this work, we aim at elucidating the atomic scale structural parameters governing the cyclic performance of MgO-based CO<sub>2</sub> sorbents. To this end, we use time-resolved (1 s) synchrotron-based *in situ* X-ray powder diffraction (XRD) to analyse the structural dynamics of a NaNO<sub>3</sub>-promoted MgO-based sorbent during cyclic operation. The sorbent was studied during 10 consecutive cycles of carbonation (90 min, 315 °C, CO<sub>2</sub>) and regeneration (15 min, 450 °C, N<sub>2</sub>) which lasted 24 hours in total (Figure 1a, carbonation cycles 1, 3, 10). A parametric Rietveld refinement was employed to quantify the evolution of the crystalline phases during the experiment. The material showed an initial deactivation during the 2<sup>nd</sup> and 3<sup>rd</sup> cycles (Figure 1b). The deactivation was followed by a re-activation during the following cycles. Turning to kinetics, also the rate of MgCO<sub>3</sub> formation exhibited an initial decrease (reduction in the kinetic rate constant as obtained via the fitting of MgCO<sub>3</sub> formation curves with the Avrami-Erofeev model) and longer induction periods in the 2<sup>nd</sup> and 3<sup>rd</sup> cycles (Figure 1c, d). The deactivation of the sorbent in the 2<sup>nd</sup> and 3<sup>rd</sup> cycles was related to the sintering of MgO, resulting in the loss of surface area (inversely proportional to the average crystallite size of MgO,  $\langle D_{\text{MgO}} \rangle^{-1}$ , Figure 1e). On the other hand, we observe the *in situ* formation of a Na<sub>2</sub>Mg(CO<sub>3</sub>)<sub>2</sub> phase (due to NaNO<sub>3</sub> decomposition and carbonation as studied by *in situ* Raman spectroscopy) with increasing content with cycle number. The reactivation of the sorbent starting with the 4<sup>th</sup> cycle correlates with the continuous increase of content of Na<sub>2</sub>Mg(CO<sub>3</sub>)<sub>2</sub> (Figure 1f). We explain the reactivation of the sorbent by the *in situ* formation of Na<sub>2</sub>Mg(CO<sub>3</sub>)<sub>2</sub> crystallites which act as effective nucleation seeds for MgCO<sub>3</sub> formation due to similarities in their crystalline structures (MgCO<sub>3</sub> (R-3c) and Na<sub>2</sub>Mg(CO<sub>3</sub>)<sub>2</sub> (R-3)). Strain effects in the MgCO<sub>3</sub> lattice along the c-axis support this hypothesis.

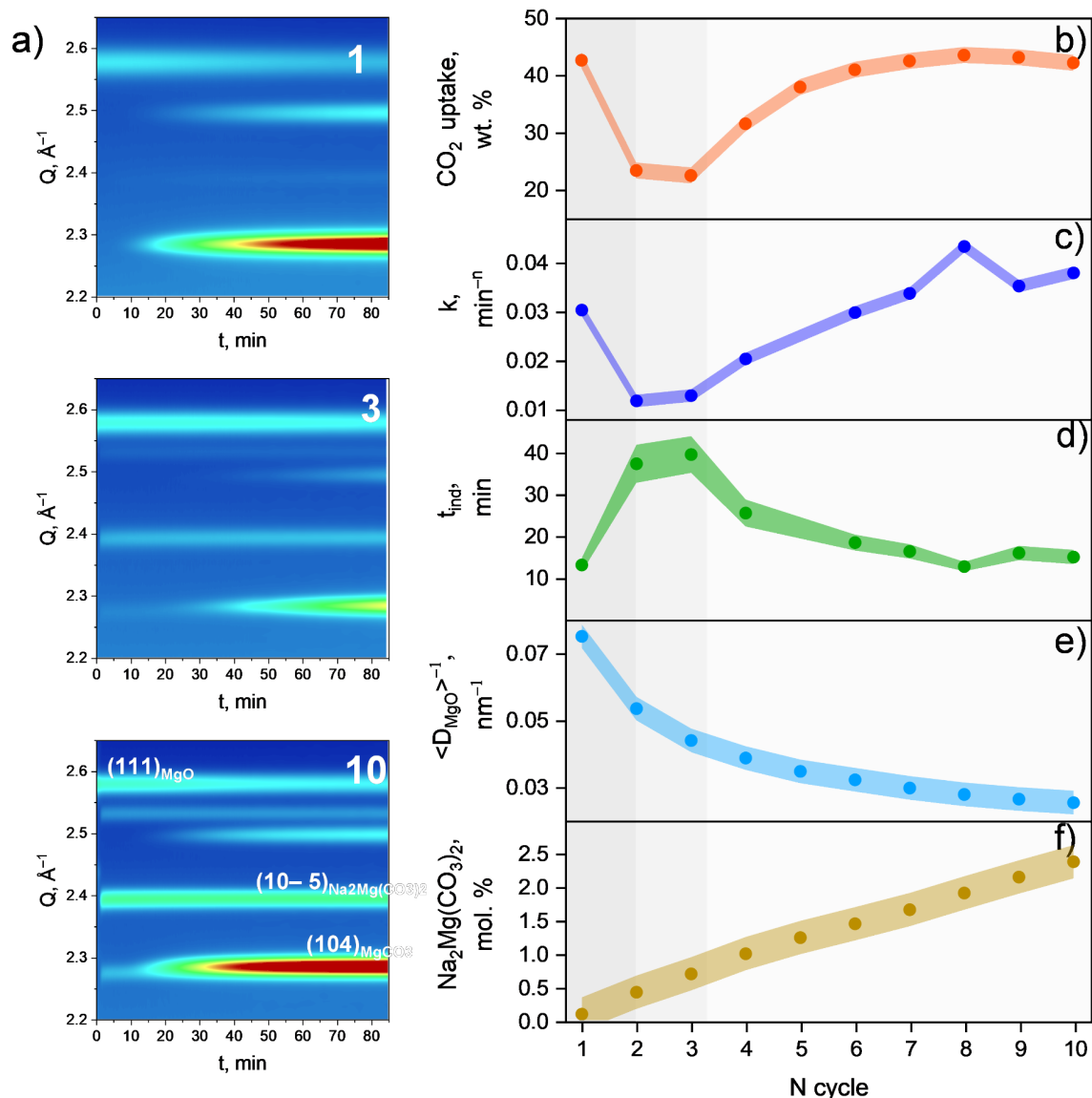


Figure 1. a) Contour plots showing the evolution of the XRD data as a function of time (t) during the 1<sup>st</sup>, 3<sup>rd</sup> and 10<sup>th</sup> carbonation cycles (315 °C, 7 ml min<sup>-1</sup> CO<sub>2</sub>), representative reflections of MgO, MgCO<sub>3</sub> and Na<sub>2</sub>Mg(CO<sub>3</sub>)<sub>2</sub> phases in the Q-range of 2.2–2.7 Å<sup>-1</sup> are labelled. Evolution of the cyclic performance of the sorbent: b) CO<sub>2</sub> uptake at t = 85 min, c) reaction rate constant (k) extracted from the kinetic modelling using the Avrami-Erofeev equation, d) induction period estimated as a time to form 3 wt.% of MgCO<sub>3</sub>, e) evolution of MgO crystallite surface to volume ratio  $\langle D_{MgO} \rangle^{-1}$ , f) fraction of Na<sub>2</sub>Mg(CO<sub>3</sub>)<sub>2</sub> at t = 5 min.

[1] Alessandro, Dal Pozzo; Andaç, Armutlulu; Margarita, Rekhtina; Paula M., Abdala; Christoph R., Müller; ACS Applied Energy Material; 2019; 2(2): 1295–1307.

[2] Hu, Yingchao; Yafei, Guo; Jian, Sun; Hailong, Li; Wenqiang, Liu; Journal of Materials Chemistry A; 2019; 7(35): 20103–20120.

[3] Chang, Ribooga; Xianyue Wu; Ocean Cheung; and Wen Liu.; Journal of Materials Chemistry A; 2022.

[4] Chen, Jian; Lunbo Duan; Felix Donat; and Christoph R. Müller.; ACS Sustainable Chemistry & Engineering; 2021; 9(19): 6659-6672.

Antonio Cervellino (1), Ruggero Frison (2)

(1) Swiss Light Source, Paul Scherrer Institut – 5232 Villigen, Switzerland. (2) University of Zurich - 8057 Zurich, Switzerland.

We have recently published a paper detailing how to deal with a non-uniform orientation distribution function (ODF) in a powder or polycrystalline sample when the full continuous angular intensity distribution is desired, as for total scattering studies. In the case with uniform ODF the intensity distribution is easily evaluated via the Debye scattering equation (DSE). A generalised form of the DSE for non-uniform ODF (texture) is presented in [1]. However, the detailed implementation depends on the scattering geometry; in [1] only the three most important experimental geometries (Bragg-Brentano, Debye-Scherrer, flat plate transmission) were considered. The geometry with grazing incidence (GI) on flat samples was not explicitly dealt with.

We have therefore derived the texture correction for total scattering functions for this geometry and its varied set of sub-cases, wherein for instance the sample is rotating around an axis normal to its exposed surface (the  $z$  axis in Fig. 1) or not, and when not, whether the  $z$  axis is still the main symmetry element for the macroscopic sample symmetry or not. We hope this effort will help total scattering studies on thin films, as for those GI is the most natural and often unavoidable geometry for diffraction experiments [2].

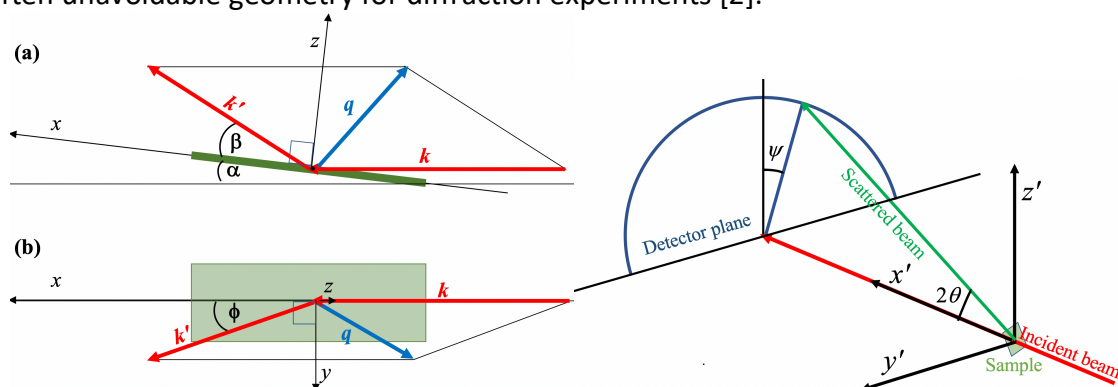


Figure 1. The geometry of grazing incidence with a 2-D detector here considered.

[1] A. Cervellino and R. Frison, *Acta Cryst.* (2020) A76, 302-317, DOI 10.1107/S2053273320002521.

[2] A.-C. Dippel, M. Roelsgaard, U. Boettger, T. Schneller, O. Gutowski and U. Ruett, *IUCr*, (2019) 6, 290–298.

# Refinement of anomalous dispersion correction parameters in single-crystal XRD

Poster  
15

Florian Meurer (1), Oleg V. Dolomanov (2), Christoph Hennig (3,4), Norbert Peyerimhoff (5), Florian Kleemiss (1), Horst Puschmann (2,5), Michael Bodensteiner (1)

(1) Faculty for Chemistry and Pharmacy, University of Regensburg, Germany, (2) OlexSys Ltd, Chemistry Department, Durham University, United Kingdom, (3) Institute of Resource Ecology, Helmholtz-Zentrum Dresden-Rossendorf (HZDR), Germany, (4) Rossendorf Beamline (BM20-CRG), European Synchrotron Radiation Facility (ESRF) Grenoble, France, (5) Department of Mathematical Sciences, Durham University, United Kingdom.

Correcting for anomalous dispersion takes the inelastic scattering in the diffraction experiment into account.[1] This X-ray absorption effect is specific to each chemical compound and particularly sensitive to radiation energies in the region of the absorption edges of the elements in the compound. The widely used tabulated values for these corrections are only approximations as they are based on calculations for isolated atoms.[2] Features of the unique spatial and electronic environment are ignored, although these can be spectroscopically observed. This significantly affects the fit between the crystallographic model and the measured. The dispersive ( $f'$ ) and absorptive ( $f''$ ) terms of the anomalous dispersion can be refined as independent parameters in the full-matrix least-squares refinement.[3] This procedure has now been implemented as a new feature in the well-established *Olex2* software suite.[4] The refined parameters are in good agreement with independently recorded X-ray absorption spectra (Fig. 1).

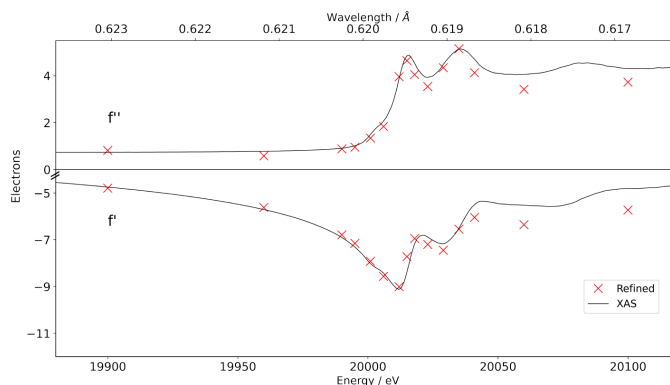


Figure 18 – Experimentally determined (black lines) and refined (red crosses)  $f'$  and  $f''$  values of  $\text{Mo}(\text{CO})_6$ .

The presentation will report on synchrotron multi-wavelength single-crystal X-ray diffraction as well as X-ray absorption spectroscopy experiments which we performed on the molecular compound  $\text{Mo}(\text{CO})_6$  at energies around the molybdenum K edge (20,000 eV). It will further show strong deviations observed with home laboratory sources even far from an absorption edge and provide an outlook into the application to determine oxidation states of organometallic compounds.

[1] S. Caticha-Ellis, *Anomalous Dispersion of X-rays in Crystallography* **1981**; [2] a) B. L. Henke, E. M. Gullikson, J. C. Davis, *At. Data Nucl. Data Tables* **1993**, *54*, 181–342; b) S. Brennan, P. L. Cowan, *Rev. Sci. Instrum.* **1992**, *63*, 850–853; c) S. Sasaki, *KEK Report* **1989**, *88*, 1–136; [3] O. Einsle, S. L. A. Andrade, H. Dobbek, J. Meyer, D. C. Rees, *J. Am. Chem. Soc.* **2007**, *129*, 2210–2211; [4] F. Meurer, O. V. Dolomanov, C. Hennig, N. Peyerimhoff, F. Kleemiss, H. Puschmann, M. Bodensteiner, *IUCrJ* **2022**, *9*, online.

# Understanding Borate Anion Induced Structural Evolution in Copper-Oxo Cluster Complexes: From In-Crystallo Transformations To Targeted Synthesis

Poster  
16

Devi Prasad Adiyeri Saseendran (1), Rangsiman Ketkaew(1), Carlos Triana (1), Sandra Lubert (1), Greta R. Patzke (1)

[1] *Department of Chemistry, University of Zurich, 8057 Zurich, Switzerland.*

Spanning from larger MOFs, and coordination complexes to smaller nanoclusters, copper-oxo clusters play an important role in the design of novel functional materials.<sup>[1-3]</sup> And the same being an integral part of energy conversion processes such as methanol generation, water splitting, and photonic devices, the strategic design of such Copper-oxo complexes is of utmost importance.<sup>[4]</sup> In this regard, understanding the formation mechanism of Cu-oxo clusters at the structural and electronic level would ultimately benefit in paving a targeted synthetic approach towards the preparation of the same, by which a chemist could acquire control over their nuclearity, cluster size, and electronic structure by applying specific chemical-synthetic tuning procedures.<sup>[5]</sup> Herein, we report the counter-anion-dependent structural evolution and related in-crystallo transformations of a novel class of Cu-oxo cluster complexes, which also serves as an active water oxidation catalyst.

With single crystal X-ray crystallographic (SC-XRD) evidence, we show that the final stable coordination state of Cu coordination complexes is highly influenced by the counter anions involved in the synthetic reaction and these anions induce in-crystallo structural transformations on these Cu-oxo complexes within the single crystal entity. Additionally, by employing in-situ X-ray Absorption Spectroscopy (XAS), we propose that tuning the electron density at the counter anion could eventually sway the Cu nuclearity in the oxo clusters, therein controlling the cluster size evolution. Furthermore, with UV-Visible spectroscopic and Mass spectral data, we confirm the heptamer to dimer to monomer transformation of these Cu-oxo cluster complexes under the presence of electronically tuned borate anions.

## References:

- [1] Z. Weng, Y. Wu, M. Wang, J. Jiang, K. Yang, S. Huo, X. F. Wang, Q. Ma, G. W. Brudvig, V. S. Batista, Y. Liang, Z. Feng, H. Wang, *Nat. Commun* 9 (2018), 1–9.
- [2] K. A. Lomachenko, E. Borfecchia, C. Negri, G. Berlier, C. Lamberti, P. Beato, H. Falsig, S. Bordiga, H. A. Topsøe, H. Topsøes Alle, K. Lyngby, *J. Am. Chem. Soc* 138 (2016), 12025–12028.
- [3] M. Langerman, D. G. H. Hetterscheid, *ChemElectroChem* 8 (2021), 2783–2791.
- [4] C. E. Elwell, N. L. Gagnon, B. D. Neisen, D. Dhar, A. D. Spaeth, G. M. Yee, W. B. Tolman, *Chem. Rev* 117 (2017), 2059–2107.
- [5] F. Song, K. Al-Ameed, M. Schilling, T. Fox, S. Lubert, G. R. Patzke, *J. Am. Chem. Soc* 141 (2019), 8846–8857.

## Synergy-ED: A new electron diffractometer for 3D-ED

Fraser White<sup>a</sup>, Akihito Yamano<sup>a</sup>, Sho Ito<sup>a</sup>, Takashi Matsumoto<sup>a</sup>, Hiroyasu Sato<sup>a</sup>, Joseph Ferrara<sup>b</sup>, Mathias Meyer<sup>c</sup>, Michał Jasnowski<sup>c</sup>, Eiji Okunishi<sup>d</sup> and Yoshitaka Aoyama<sup>d</sup>

a. Rigaku Corporation, Haijima, Tokyo, Japan

b. Rigaku Americas Corporation, The Woodlands, Texas, USA

c. Rigaku Polska, Wrocław, Poland

d. JEOL Ltd., Akishima, Tokyo, Japan

The study of the structure of single crystals is typically achieved with X-ray diffraction. Many decades of progress in instrumentations have pushed the limits of the technique, and the current generation of home lab instruments allows the study of crystals down to about 1 micron in size, rivalling synchrotrons. In the quest to analyse even smaller samples than this, three-dimensional electron diffraction (3D-ED), also known as microcrystal electron diffraction (MicroED) has become increasingly popular in recent years.<sup>1</sup> Leveraging the high interaction strength and weaker damage effects of electron radiation<sup>2</sup>, solving structures of sub-micron crystallites of all classes of samples becomes possible. Thus far, most 3D-ED experiments have been conducted by specialized research groups in transmission electron microscopes (TEMs), requiring hard- and software modifications, and a high skill level in both microscopy and crystallography.

Leveraging their expertise in integrated crystallography solutions and electron beam devices, Rigaku and JEOL joined forces to develop a fully integrated hard- and software solution for 3D-ED: the XtaLAB Synergy-ED.<sup>3</sup> Its hardware comprises a JEOL electron gun and beamline specifically tailored to reliably obtaining optimal crystallography results, and a Rigaku HyPix-ED hybrid-pixel diffraction detector which allows noise-free data collection with high speed and dynamic range. Both components are fully integrated into CrysAlis<sup>Pro</sup>, the comprehensive, user-inspired data collection and processing software platform as also used on Rigaku's single-crystal diffractometers. Its evolved, streamlined workflow from instrument control to structure solution allows crystallographers to readily conduct 3D-ED experiments without any involved instrumentation setup or prior knowledge of electron microscopy and diffraction.

We will present the latest technological developments of the Synergy-ED platform, as well as discuss results from our application laboratories on various classes of samples and measurement modalities.

1. Gemmi, M. *et al.* 3D Electron Diffraction: The Nanocrystallography Revolution. *ACS Cent. Sci.* **5**, 1315–1329 (2019).
2. Clabbers, M. T. B. & Abrahams, J. P. Electron diffraction and three-dimensional crystallography for structural biology. *Crystallogr. Rev.* **24**, 176–204 (2018).
3. Ito, S. *et al.* Structure determination of small molecule compounds by an electron diffractometer for 3D ED/MicroED. *CrystEngComm* **23**, 8622–8630 (2021).

## Structural evolution of polyiodides at high pressure

Poster  
18

Tomasz Poręba (1), Mohamed Mezouar (1), Stefano Racioppi(2)

[1] European Synchrotron Radiation Facility, 71 Avenue des Martyrs, 38000 Grenoble, France

[2] Department of Chemistry, State University of New York at Buffalo, Buffalo, 14260-3000 New York, United States

Polyiodides are known to form extensive homoleptic assemblies in solid state: from linear iodine chains to complex three-dimensional cages. A large variety of polyiodide structures stem from the high bonding flexibility of iodine, usually attributed to the formation of multicenter bonding. Herein, we show how pressure affects the structure and physicochemical properties of two polyiodides: archetypical asymmetric triiodide in  $\text{CsI}_3$ , and organic donor-acceptor system of tetraethylammonium diiodine triiodide – for which both high-pressure structures were studied by single-crystal X-ray diffraction.

In the first, dominant PV term favours more symmetric phase above 1.24 GPa. Upon phase transition, iodine herringbone motif turns to orthogonal linear chains made of  $(\text{I}_3^-)_n$ . Theoretical calculations show that upon compression, there is electron density shift from the intramolecular region into intermolecular one. The whole process is accompanied by a bandgap closure. However, electrical resistivity experiments did not show any abrupt changes in material resistivity at high pressure.

In the second example, pressurization above 10 GPa forces  $\text{I}_2$  and  $\text{I}_3^-$  units to as close as 3.2 Å. At this separation, this organic salt show a dramatic drop in electrical resistivity by 9 orders of magnitude. Raman spectroscopy shows progressive quenching of the stretching vibration mode of iodine, which is interpreted as a formation of a polymeric system.

[1] T. Poręba, M. Ernst, D. Zimmer, P. Macchi, N. Casati, *Angew. Chem. Int. Ed.* **2019**, 58, 6625

[2] T. Poręba, S. Racioppi *et al*, *Inorg. Chem.* **2022**, 61, 28, 10977–10985

## In-situ optical spectroscopy of crystallization: one crystal nucleation at a time

Oscar Urquidi(1)<sup>†</sup>, Johanna Brazard(1)<sup>†</sup>, Natalie LeMessurier(2), Lena Simine(2), Takuji B. M. Adachi(1)

(1) Department of Physical Chemistry, Sciences II, University of Geneva, 30, Quai Ernest Ansermet, 1211 Geneva, Switzerland

(2) Department of Chemistry, McGill University, 801 Sherbrooke Street W, Montreal, Quebec H3A 0B8, Canada

<sup>†</sup> These authors contributed equally to this work

Crystallization is an important process in many scientific and industrial disciplines. After decades of research, the fundamental understanding of crystal nucleation at the molecular level has yet to be established. Recent studies agree that the process of crystal nucleation is more complex than what the classical nucleation theory describes. Although In-situ optical spectroscopy has the potential to collect complex information from nucleation dynamics, its application has been limited by the stochastic and heterogeneous nature of crystal nucleation. Single molecule spectroscopy carries a powerful and well-established concept to tackle the study of stochastic, complex, and heterogeneous systems. Translating this concept to the study of crystal nucleation, optical spectroscopy can be used in its full potential by probing a single nucleation event at a time, if we can accurately predict its location.

In our work[1], we present the development of Single Crystal Nucleation Spectroscopy (SCNS), which aims to perform in situ optical spectroscopy of crystal nucleation. SCNS is based on a novel combination of Optical Trapping Induced Crystallization (OTIC) and Raman micro-spectroscopy. Demonstrated in 2007 by Sugiyama et al.[2], OTIC was first performed by focusing a near-infrared (NIR) laser in a supersaturated glycine/D2O solution. In our approach, we applied OTIC to spatially control a single nucleation event at the laser focus, while simultaneously measuring the Raman spectral evolution. We acquired the Raman spectral evolution of a single glycine crystal formation in aqueous solution at room temperature, with a time resolution of 46 ms. Raman spectral evolution acquired during single nucleation events was analyzed by an unsupervised spectral decomposition technique, and revealed that nucleation occurs through a nonclassical mechanism, which led us to obtain the Raman spectrum of pre-nucleation aggregates. The agreement between the simulated and experimentally extracted spectra of pre-nucleation aggregates allowed us to assign loosely bound linear glycine chains as likely precursors of crystal formation. While providing us with more details about the early stages of glycine nucleation process, our results also underline the power of SCNS as a platform for the study of crystallization by means of optical spectroscopy.

[1] O. Urquidi, J. Brazard, N. LeMessurier, L. Simine, and T. B. M. Adachi, Proc. Natl. Acad. Sci. U.S.A., vol. 119, no. 16, p. e2122990119, Apr. 2022, doi: 10.1073/pnas.2122990119.

[2] T. Sugiyama, T. Adachi, and H. Masuhara, Chem. Lett., vol. 36, no. 12, pp. 1480–1481, Dec. 2007, doi: 10.1246/cl.2007.1480.

Joohee Bang<sup>1</sup>, Nives Strkalj<sup>2</sup>, Martin Sarott<sup>1</sup>, Morgan Trassin<sup>1</sup>, Thomas Weber<sup>1</sup>

<sup>1</sup>Department of Materials Science, ETH Zurich, Switzerland

<sup>2</sup>Department of Materials Science and Metallurgy, Cambridge University, United Kingdom

Ferroelectric thin films have attracted great attention for its rich applications in energy-efficient electronic devices because of their relevant physical properties such as high dielectric constants, electrically switchable polarization, and high piezoelectric coefficients\*. In fact, the growing demand for miniaturized microelectronics has inspired diverse research efforts towards the engineering of ferroelectric properties and domain architectures in the ultrathin regime†. Thus, comprehending the structural and electrical properties of ferroelectric thin films on the nanoscale became crucial. Recently, a lot of effort has been put into studying ferroelectric oxide superlattices with complex topologies such as long-range vortex-antivortex arrays of polarization‡. These works have called for an in-depth structural investigation of the superlattice structures, since the orientation and arrangement of ferroelectric domains define the macroscopic ferroelectric properties in ferroelectric thin films. Here, we report on a newly discovered local order state in superlattices consisting of ferroelectric lead titanate and dielectric strontium titanate using a complete three-dimensional diffuse X-ray scattering data analyzed with 3D- $\Delta$ PDF method§. The data was collected with single crystal diffuse X-ray scattering technique, which, to the best of our knowledge, was used for the first time to study local order in single crystalline thin films. This work will not only contribute to gaining useful insights on structure-property correlations of ferroelectric oxide superlattices, but also lay groundwork for developing a novel non-disruptive solid-state characterization technique for analyzing local structures of thin films.

---

\* Setter, N., et al. "Ferroelectric thin films: Review of materials, properties, and applications." *Journal of applied physics* 100.5 (2006): 051606

† Fong, Dillon D., et al. "Ferroelectricity in ultrathin perovskite films." *Science* 304.5677 (2004): 1650-1653; Kornev, Igor A., et al. "Ferroelectricity of perovskites under pressure." *Physical review letters* 95.19 (2005): 196804; Schlom, Darrell G., et al. "Strain tuning of ferroelectric thin films." *Annu. Rev. Mater. Res.* 37 (2007): 589-626.

‡ Yadav, A. K., et al. "Observation of polar vortices in oxide superlattices." *Nature* 530.7589 (2016): 198-201; Damodaran, Anoop R., et al. "Phase coexistence and electric-field control of toroidal order in oxide superlattices." *Nature materials* 16.10 (2017): 1003-1009; Das, S., et al. "Observation of room-temperature polar skyrmions." *Nature* 568.7752 (2019): 368-372.

§ Weber, Thomas, and Arkadiy Simonov. "The three-dimensional pair distribution function analysis of disordered single crystals: basic concepts." (2012): 238-247.

M. Adam<sup>2</sup>, A. Abboud<sup>2</sup>, R. Durst<sup>2</sup>, J. Graf<sup>1</sup>, C. Michaelsen<sup>1</sup>, T. Stuerzer<sup>2</sup>

<sup>1</sup>Incoatec GmbH - Geesthacht (Germany), <sup>2</sup>Bruker AXS GmbH - Karlsruhe (Germany)

The structure determination on ever smaller and more weakly diffracting crystals is one of the biggest challenges in crystallography. Traditionally, in-house X-ray crystallography covers sample sizes down to a lower limit of approximately 50  $\mu\text{m}$ . Consequently, electron diffraction is receiving a lot of attention, as electron diffraction methods promise structure determination on significantly smaller samples. However, while micro-ED can cope with samples in the nm regime, an upper limit in the range of approximately 1  $\mu\text{m}$  exists. At the same time crystallization of suitably small crystals can be difficult and grinding larger samples to bring them into suitable sizes can add a severe threat to electron diffraction methods. On the other hand, the formation of crystals in sizes of the few micrometers often can be easily accomplished. Equipment for structure determination closing the gap for samples between 50 to 1 micrometer in size would be highly desirable.

Fortunately, the 50 micron 'limit' for in house X-ray diffraction is not a hard border anymore. At Bruker and Incoatec we are continuously exploring the technical restrictions of X-ray diffraction instrumentation in order to find ways to push or even overcome some of the limitations. This holds for all elements in a system, and in particular for main components, such as detectors, sources, and goniometers.

For detectors new methods of photon-counting are paving the way to reliably collect data from ever smaller samples. Conventionally, photon-counting detectors have operated in the time domain, in which X-rays are counted one-by-one as they hit the detector. However, this type of serial detection has limitations. It has been proposed that photon counting in the space domain should have significant advantages. In this approach the detector produces a fast 'movie' of the evolving X-ray diffraction pattern and then a processor looks for individual events in each frame of the movie. We will demonstrate the advantages of space-domain versus time-domain photon counting and explain how space-domain photon counting can be implemented using the latest generation of real-time processors. We also will shine light on which recent improvements made the new generation of detectors possible.

On the source side, modern low power microfocus X-ray sealed tube sources define the state-of-the-art for in-house X-ray diffraction equipment, as they deliver intensities in the range of rotating anodes yet maintain all the comfort of a sealed tube system. Recent improvements in the heat transfer of the anode - using diamond with its about 8 times higher heat conductivity compared to copper - are leading to brighter X-rays sealed tube microfocus X-ray sources.

Improvements in the detector and source technology must be reflected by all other components to finally form the diffraction solution for the small samples under discussion. This holds for goniometer stability and accuracy and is finally completed by devices such as automated motorized goniometer heads, carefully maintaining the crystal in the center of the X-ray beam. The latest generation of the D8 QUEST and D8 VENTURE features the new outstanding components and comes along with the fully featured, easy to use APEX or PROTEUM software suits.

With these systems in their lab crystallographers are nowadays routinely able to successfully determine the structure on samples significantly smaller than 50 microns. Often samples exhibiting a single digit micron size can be successfully investigated.

We will discuss the latest innovations and present selected results from crystallography.